Electronic Thesis and Dissertation Repository

10-6-2021 2:00 PM

Comparison of geosmin and 2-methylisoborneol removal by conventional ozonation and co-treatment of potassium ferrate and peroxymonosulfate

Zhaoran Xin, *The University of Western Ontario*

Supervisor: Rehmann, Lars, *The University of Western Ontario*
Co-Supervisor: Ray, Madhumita, *The University of Western Ontario*
A thesis submitted in partial fulfillment of the requirements for the Master of Engineering Science degree in Chemical and Biochemical Engineering
© Zhaoran Xin 2021

Recommended Citation

Abstract

Geosmin and 2-methylisoborneol (2-MIB) are two common compounds that cause taste and odor problems in water. This study compares geosmin and 2-MIB removal from water by conventional ozonation, ferrate and peroxymonosulfate (PMS) oxidation processes. The effects of initial O_3 doses, H_2O_2/O_3 ratios, and pH on the removal efficiency of geosmin and 2-MIB were evaluated for ozonation. The addition of H_2O_2 and alkaline condition increased the removal efficiency by ozonation. A Box-Behnken Design was applied to study the influence of ferrate and PMS dosage and pH on the removal of geosmin. It was shown that Ferrate alone was not effective for removing geosmin, but the co-treatment of ferrate and PMS can achieve good geosmin removal.

Keywords

Geosmin and 2-methylisoborneol; Ozonation; peroxymonosulfate and ferrate; advanced oxidation process

Summary for Lay Audience

Two of the most common chemicals in drinking water causing unpleasant odors are geosmin and 2-Methylisoborneol (2-MIB). Removal of these two chemicals is challenging for two main reasons. Firstly, the human ability to notice geosmin and 2-MIB is excellent. It means that removal methods are unsuccessful even if only a trace amount of these two chemicals remained after the treatment. Another reason is that geosmin and 2-MIB are resistant to conventional removal processes, including ozonation and absorption. To have better removal results, more potent chemicals are used to oxidize these two compounds. Such removal technologies are called advanced oxidation processes (AOPs). In AOPs, radicals including $\cdot OH$, $\cdot SO_4^-$ or $\cdot FeO_4^-$ are generated to degrade pollutants.

Firstly, this research examined a traditional AOP method, ozonation. The results showed the addition of ozone was not efficient in the removal of the target pollutants. This was likely due to insufficient ozone dosage and the scavenging effect of methanol (used as a solvent to dissolve geosmin and 2-MIB). Furthermore, the addition of H_2O_2 and an alkaline environment can increase the removal efficiency.

To achieve better removal, the co-treatment of ferrate and peroxymonosulfate (PMS) was studied. Parameters including pH and dosage of PMS and ferrate were investigated. The results showed that this co-treatment process can remove geosmin completely.

Further research could be conducted to investigate the principle of the co-treatment process and the reason for the inefficiency of ferrate oxidation of geosmin and 2-MIB.

Co-Authorship Statement

Chapter 2

Zhaoran Xin: Designed and conducted experiments, analyzed samples, interpretation of data, and writing

Dr. Lars Rehmann: Supervised the research work, assisted in data analysis, editing

Dr. Madhumita B. Ray: Supervised the research work, assisted in data analysis

Chapter 3

Zhaoran Xin: Designed and conducted experiments, analyzed samples, interpretation of data, and writing

Dr. Lars Rehmann: Supervised the research work, assisted in data analysis, editing

Dr. Madhumita B. Ray: Designed experiments, supervised the research work

Chapter 4

Zhaoran Xin: Designed and conducted experiments, analyzed samples, interpretation of data, and writing

Dr. Lars Rehmann: Editing

Dr. Madhumita B. Ray: Supervised the research work, editing

Acknowledgments

I would like to thank Dr. Lars Rehmann and Dr. Madhumita B. Ray for helping and their support.

I would also like to thank all my friends and my family.

I really appreciate my best friend William who supported me and helped me all the time.

Table of Contents

List of Tables

List of Figures

Chapter 1

1.   Literature review

1.1   Introduction

Based on the following literature studies, potassium ferrate (PF) and peroxymonosulfate (PMS) co-treatment has been applied as an innovative method for the elimination of lignocellulosic, fluoroquinolones, and atrazine (Feng et al., 2017; Wang et al., 2020; Wu et al., 2018). However, this has not been applied in the degradation of taste and odor compounds.

In this work potential treatment method with co-treatment of PMS and PF for removal of geosmin and 2-methylisoborneol (2-MIB) is proposed. The performance of this method will be compared with the commonly applied ozonation and combination of ozonation and hydrogen peroxide. The effects of operating conditions such as dosage of oxidants, pH, and initial concentration of geosmin and 2-MIB will be determined.
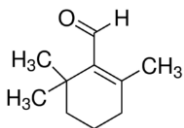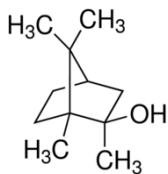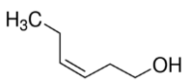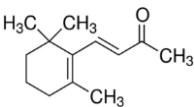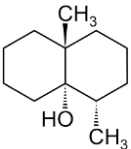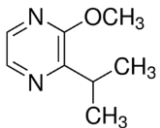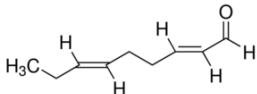
The effect of PMS and PF dose will be investigated in batch systems. The kinetics and efficiencies of geosmin and 2-MIB deduction will be compared for conventional ozonation and co-treatment of PMS and PF.
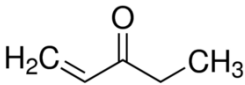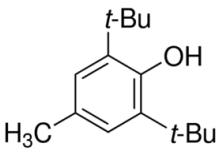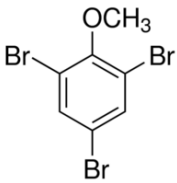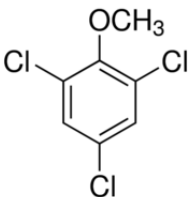
1.2   Off-flavor

Off-flavor in water results from undesirable taste and odor (T&O) compounds, and it is an important parameter of water quality according to WHO (Kimstach, 1992). Table 1.1 shows common T&O compounds in water. A survey of 59 Great Lakes drinking water treatment plants reported that 20% of the plants experienced severe taste and odor problems annually (Watson et al., 2008). In the US, bottled water plants face $813 million annually to deal with the off-flavor (Dodds et al., 2009).

In addition to drinking water, wineries (Cortada et al., 2011), aquaculture (Rodriguez-Gonzalez et al., 2019), food processing, and wastewater treatment plants (Agus et al., 2012) also suffer from off-flavor issues.
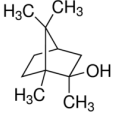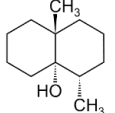
Table 1.1 Common odor components in water (Peter & Von Gunten, 2007)

Compound (CAS number)	Structure	Odor	Odor threshold (ng L^{-1})	Source
β-cyclocitral (432-25-7)		fruity	19000	cyanobacteria
2-Methylisoborneol (2371-42-8)		musty	15	cyanobacteria and actinomycetes
cis-3-hexen-1-ol (928-96-1)		grassy	70000	algae
β-ionone (14901-07-6)		violets	7	algae, cyanobacteria
Geosmin (19700-21-1)		earthy	4	cyanobacteria and actinomycetes
2-isopropyl-3-methoxypyrazine (25773-40-4)		decaying vegetation	0.2	actinomycetes
trans, cis-2,6-nonadienal (17587-33-6)		cucumber	20	algae

1-penten-3-one (1629-58-9)		fishy-rancid	1250	algae, cyanobacteria
2,6-di-*tert*-butyl-4-methylphenol (BHT) (128-37-0)		plastic	Not available	leaching from polyethylene pipes
2,4,6-tribromoanisole (TBA) (607-99-8)		earthy-musty	0.03	methylation of bromophenol by microorganisms
2,4,6-trichloroanisole (TCA) (87-40-1)		musty	0.03	methylation of bromophenol by microorganisms
Chlorine		bleach chlorinous, medicinal		

Off-flavors cause significant economic problems in aquaculture due to repulsive odor or taste in fish. Off-flavors in fish have been studied extensively in catfish, tilapia, salmon, and trout (Robertson and Lawton, 2003) and the problem of earthy/musty odors and tastes is related to geosmin and 2-methylisoborneol (2-MIB) in fish flesh (Tucker, 2000).

Table 1.2 Properties of 2-MIB and geosmin

	2-Methylisoborneol	Geosmin	Reference
Molecular formula	$C_{11}H_{20}O$	$C_{12}H_{22}O$	
Odor	musty	earthy	
Structure			
Molecular weight ($g \cdot mol^{-1}$)	168.28	182.307	
Boiling point (°C at 760 mmHg)	207 to 209	270 to 271	
Density ($g \cdot cm^{-3}$)	0.9288	0.9494	
Solubility ($g \cdot L^{-1}$)	0.45	0.051	ALOGPS
pKa	-0.42	-0.0047	ChemAxon
log P	3.25	3.66	ALOGPS
log Kow	3.31	3.57	(Howgate, 2004)
Vapor pressure (Pa)	6.68	5.49	(Clercin, 2019)
Henry's law constant (atm-m^3/mole)	5.76	6.66	(Clercin, 2019)

These two earthy/musty flavor compounds in water and fish are from cyanobacteria and actinomycetes (Zimba et al., 2001). These microorganisms develop during the summer and the beginning of the fall, and to some extent in the spring (Jensen, 1988).

1.3   Geosmin and 2-MIB

The musty/earthy odor smelled in the air during and rainfall after a long draught is mainly from geosmin and 2-methyl-isoborneol (2-MIB) (Jelen Ä et al., 2003). The smell of these compounds is prominent because humans are sensitive to trace amounts of geosmin and 2-MIB, with odor threshold concentrations (OTC) of 10 ng·L^{-1} and 4 ng·L^{-1}, respectively (Guo et al., 2016). Table 1.2 shows the properties of 2-MIB and geosmin.

1.3.1   Cyanobacteria and actinomycetes

Benthic cyanobacteria are responsible for producing geosmin and 2-MIB, for example, Phormidium produces 2-MIB, and geosmin is produced by *Oscillatoria* and *Phormidium, Pseudanabaena* (Xia et al., 2020).

The cyanobacteria blooms occur at certain conditions, including slow-moving water, warm temperature, neutral to alkaline pH (pH 6 to 9), and increasing nutrient availability (Bellu, 2007). The extra nutrient often comes from upstream water polluted by industry wastewater, fertilizer, or septic tank. In addition, by global climate change, the increasing number of these microbes has become a severe issue for agriculture.

Another minor contributor to the off-flavor is actinomycetes (Zuo et al., 2009), generally present in soil and bank debris or bottom mud in rivers. The smell is washed into water (Bellu, 2007). Furthermore, actinomycetes can also be present in vegetables like beetroot (Aeree et al., 1976) or colonize on malts, casks, and cork in the winery (Lee et al., 2001), which leads to the foul smell of beetroot or wine during storage.

Table 1.3 Detected geosmin and 2-MIB concentrations in reservoir and wastewater

Source	Geosmin ($\mu g \cdot L^{-1}$)	2-MIB ($\mu g \cdot L^{-1}$)	Location	Reference
Reservoir	0.25–15.43	0.14–35.48	Southwest of Shanghai, China	(Xia et al., 2020)
	0.03-0.04	0.03-0.04	South East Queensland, Australia	(Doederer et al., 2019)
River	0.086-0.121	0.071-0.099	Yodo River located in Kansai region in Japan	(Mizuno et al., 2011)
	<0.01	0.14	Huangpu River	(Ma et al., 2007)
Wastewater	0.025±0.006	0.013±0.008	-	(Agus et al., 2012)
Sludge supernatant from water treatment plant	5.015	9.415	South Australia	(Zamyadi et al., 2015)

1.3.2   Occurrence of GSM and 2-MIB

The concentration of odor compounds depends on the number of microbes. It varies due to environmental conditions such as season, location, and source of water. The following table shows the different concentrations of T&O compounds from various sources.

Table 1.4 Detected geosmin and 2-MIB concentrations in different food

Source	Geosmin ($\mu g \cdot kg^{-1}$)	2-MIB($\mu g \cdot kg^{-1}$)	Reference
Fish fillet	0.703±0.493	0.008±0.008	(Houle et al., 2011)
Beetroot	9.69±0.22 to 26.7±0.27		(Lu et al., 2003)
Grain	0.01 to 7.57	0.04-0.16	(Jelen Ä et al., 2003)

1.4   Analytical methods for geosmin/2-MIB

Geosmin and 2-MIB can be separated by gas chromatography (GC) due to the volatility of odor compounds (Callejón et al., 2016). Alternatively, ion mobility spectrometry (IMS) can be used for faster separation (Handy et al., 2000).

As for analysis, methods based on ionization, including mass spectrometer (MS), flame ionization detector (FID) (Romero et al., 2007), and IMS are used to quantify geosmin. UV-IMS has been applied successfully to monitor the concentration of flavor compounds during beer fermentation (Vautz et al., 2004).

To analyze T&O in field, a portable device based on differential ion mobility spectrometry (DMS) is applied. DMS has a higher electric field than IMS. The charged ions are blown by carrier gas flow and move through a field-based drift tube. The selected ion is separated by an asymmetric electric field (Camara et al., 2013).

The current trend in the industry is the use of microscale DMS (µDMS), also called FAIMS. It is cheaper, faster and portable (Aliaño-González et al., 2018). It results from the drift tube of FAIMS in a flat plate structure rather than a metal ring structure. GC-µDMS can measure geosmin in 30 s, at 7 ng·L^{-1}, lower than the human olfactory threshold, 50 ng·L^{-1} (Camara et al., 2013).

1.5   Methods to remove geosmin/2-MIB

1.5.1   Adsorption by activated carbon

Granular activated carbon (GAC) (Drikas et al., 2009; Li, 2015; Scharf et al., 2010) and powdered activated carbon (PAC) (Cook et al., 2001; C. Kim et al., 2014; Lalezary-Craig et al., 1988) are applied to adsorb taste and odor. Particularly, GAC is promising since it adsorbs most extracellular flavors compared with PAC (Zamyadi et al., 2015).

Moreover, super-powdered activated carbon (S-PAC) removes more geosmin and adsorb faster. This is because S-PAC has finer carbon particles than PAC, the mass transfer efficiency of adsorbed particles is dominated by micropore diffusion, which is more efficient than intraparticle diffusion (Matsui et al., 2009).

However, in a natural water matrix, a smaller pore size may result in less efficient adsorption of 2-MIB and geosmin due to the competition of dissolved natural organic matter (NOM) in water. The NOM molecules block the active sites and reduce the adsorption capacity. The removal efficiency of geosmin and 2-MIB in reservoir water decreased by 80 % compared to pure water at a certain dose of PAC (Zoschke et al., 2011).

In addition to pore size, the carbon properties also influence the adsorption efficiency. 2-MIB and geosmin are hydrophobic, so less-hydrophilic activated carbons are better for their removal (Matsui et al., 2015).

1.5.2   Membrane filtration

During the membrane filtration process, water passes through the membrane to separate contaminants based on different pore sizes. Nanofiltration (NF) membrane has a pore size

ranging from 0.5-10 nm. NF membrane can filter dissolved metals, salts, and T&O compounds (Pestana et al., 2020).

The effective removal of geosmin and 2-MIB was observed by the NF membrane (Zat & Benetti, 2011). Specifically, the removal efficiency by low molecular weight cut-off (MWCO) NF membranes is better than high MWCO NF membranes. However, the presence of algal metabolites in natural water may cause membrane fouling (Dixon et al., 2010; Dixon et al., 2011).

1.5.3   Microbial Treatment

Biological treatment degrades organic compounds by small organisms. It has the advantage of low investment and low cost, easy maintenance, and less possibility of contamination by the addition of chemicals or produced by-products (Xue et al., 2012).

Geosmin and 2-MIB are biodegradable because their structures are similar to alicyclic alcohols and ketones (Rittmann, 1995; Ho et al., 2007). Biofloc technology applied in suspended growth reactors (BFT-SGRs) using *Bacillus subtilis* removed 94% of geosmin and 97% of 2-MIB in recirculating aquaculture systems (RASs) (Luo et al., 2016). However, nitrogen in fish waste is reused at the same time. It may lead to nutrient over-dosing.

Therefore, a moving-bed biofilm reactor (MBBR) was designed to control the biofilm growth. MBBR achieved around 90% removal of MIB and geosmin due to the synergetic effect of biodegradation and sorption of biofilm as a carrier (Katrin Doederer et al., 2019).

Instead of a complex reactor, a biological sand filter can also remove geosmin and 2-MIB thoroughly (Doederer et al., 2018; McDowall et al., 2009; Nerenberg et al., 2000). For instance, a slow sand filter (SSF) removes $63 \pm 7\%$ of MIB and $93 \pm 3\%$ of geosmin within one day (Hsieh et al., 2010).

These filters often use GAC, PAC, or sand as support for biofilm. When the adsorption capacity of PAC or GAC is exhausted, biofilm is formed on the surface of PAC or GAC. Hence they were converted into biological activated carbon (BAC) (Kim et al., 2014).

To determine the biodegradation rate, a non-porous medium such as sand is used to avoid GAC adsorption. The results show that the biodegradation is pseudo-first-order (Ho et al., 2007), depending on the initial concentration of microbial inoculum. In contrast, biodegradation is a second-order reaction in the presence of a large amount of NOM (Rittmann, 1995).

Besides the effect of NOM, biological treatment time is much longer if the microbes have not been exposed to geosmin and 2-MIB before. In the sand filter experiment, the microbes took 22 days to acclimate and one more month to remove the compounds completely (Ho et al., 2007). A similar lag time also is observed using SSF (Hsieh et al., 2010).

To investigate the degradation mechanism of microbes, they are screened from the biofilm on a sand filter. The result shows that microbial degradation utilizing geosmin as a single carbon source is difficult. But the reaction accelerates with multiple carbon sources, for example, the addition of ethanol (Saito et al., 1999) and 2-MIB (Xue et al., 2012). This may be explained by co-metabolism. During the reaction, some enzymes are activated by various carbon sources.

Though biological treatment can remove T&O compounds lower than the detection limit, extra time is required to acclimate the microbes. The long reaction time may restrict the application if the T&O problem happens occasionally. A faster treatment is needed.

1.6 Advanced oxidation processes (AOPs)

AOPs generate highly reactive radicals, including hydroxyl radicals, as shown in Table 1.5. Hydroxyl radical reacts nonselectively with organic compounds (Staehelin & Holgné, 1982) which are resistant to conventional oxidation methods (Table 1.6).

Table 1.5 Relative oxidation activity of common oxidizing agents (Munter, 2001)

Oxidizing agent	Relative oxidation activity
Positively charged hole on titanium dioxide, TiO_2^+	2.35
Hydroxyl radical	2.05
Atomic oxygen	1.78
Ozone	1.52
Hydrogen peroxide	1.31
Permanganate	1.24
Hypochlorous acid	1.1
Chlorine	1

Table 1.6 Reaction rate constants for ozone and hydroxyl radical for organic compounds (Munter, 2001)

Organic compound	Rate constant [$M^{-1} s^{-1}$]	
	O_3	$HO\cdot$
Alcohols	10^{-2}-1	10^8-10^9
Aromatics	1-10^2	10^8-10^{10}
Chlorinated alkenes	10^3-10^4	10^9-10^{11}
Ketones	1	10^9-10^{10}
N-containing organics	10-10^2	10^8-10^{10}
Phenols	10^3	10^9-10^{10}

AOPs are widely used in wastewater treatment. In addition to the degradation of extra chemical compounds directly, AOPs are used to degrade cellular contents of pathogens to disinfect wastewater with high organic nature in the dairy industry (Afsharnia et al., 2018).

However, AOPs are capital-intensive since they include the investment of expensive reagents such as ozone and hydrogen peroxide and the cost of equipment, including ultraviolet light. Hence AOPs are often combined with traditional treatments to overcome this drawback.

1.6.1 Mechanism of AOP based on hydroxyl radical

Table 1.7 Classification of hydroxyl radical reactions with organic and inorganic compounds in AOP

Mechanism	Reaction	Reactant
Radical addition	$R + HO\cdot \rightarrow ROH$	Unsaturated or aliphatic organic compound
Hydrogen abstraction	$R\text{-}H + HO\cdot \rightarrow R\cdot + H_2O$	Alkane (Tully et al., 1986)
Electron transfer	$R^{n+} + HO\cdot \rightarrow R^{n+1+} + HO^-$	Inorganic ions

Hydroxyl radical degrades organic species of different nature. The intermediates are shown in Table 1.7 (Huang et al., 1993). Moreover, radical combination accelerates regeneration of oxidant H_2O_2.

$$HO\cdot + HO\cdot \rightarrow H_2O_2 \tag{1}$$

However, scavengers such as carbonate, bicarbonate, etc. deplete hydroxyl radicals, reducing the reaction rate (Alaton et al., 2002). The following methods are used to increase the concentration of effective HO· or other radicals or accelerating their regeneration.

1.6.2   Ozonation

Ozonation is one of the powerful AOPs. Ozonation has the advantage of being environment friendly since its residues are nontoxic, and excess ozone can be destructed into oxygen and water (Sarayu et al., 2007; de Souza et al., 2010). Among many different AOPs, ozonation is one of the most used methods in water and wastewater plants for tertiary treatment and disinfection. It is also easy to retrofit ozone in treatment plants.

Ozone reacts with organic contaminants directly or with generated hydroxyl radical indirectly.

Direct pathway (Munter, 2001)**:**

$$O_3 + R \rightarrow RO + O_2 \tag{2}$$

Indirect pathway (Beltran, 2003)**:**

$$O_3 + HO^- \rightarrow HO_2^- + O_2 \tag{3}$$

$$O_3 + HO_2^- \rightarrow HO_2\cdot + O_3^-\cdot \tag{4}$$

$$O_3^-\cdot + H^+ \rightarrow HO_3\cdot \tag{5}$$

$$HO_3\cdot \rightarrow HO\cdot + O_2 \tag{6}$$
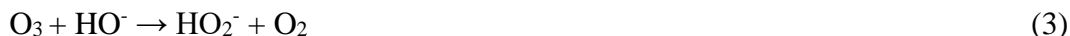
Indirect pathway overcomes the disadvantages of direct pathway, including the selectivity of ozone and its low solubility and stability (Fe-based). There are several factors, which influence the transformation of these two pathways.

Ozone reacts with compounds containing conjugated double bonds at low pH, such as C=C, C=N, N=N (Gogate & Pandit, 2004). With increasing pH, ozone decomposes faster and produces a greater amount of hydroxyl radicals by indirect pathway. Furthermore, another method to accelerate ozone decomposition is the addition of chemicals such as hydrogen peroxide, called peroxone process. The addition of H_2O_2 can increase 50% of the hydroxyl radical yield. The mechanism is listed as following equations (Fischbacher et al., 2013).

$$HO_2^- + O_3 \rightleftharpoons HO_5^- \tag{7}$$

$$HO_5^- \rightarrow HO_2\cdot + O_3^-\cdot \quad \text{or} \quad HO_5^- \rightarrow 2\,O_2 + OH^- \tag{8}$$

$$O_3^-\cdot \rightleftharpoons O_2 + O^-\cdot \tag{9}$$

$$O^-\cdot + H_2O \rightleftharpoons HO\cdot + OH^- \tag{10}$$

Catalytic ozonation has been widely studied, such as ZSM5 zeolites loaded with metallic (Ce, Fe, or Mn) (Chen et al., 2018), Fe-based catalyst (Wang & Bai, 2017), and Ni-based layered double hydroxides (Ni-LDHs) nanomaterials (El Hassani et al., 2019). Ozonation can remove geosmin and 2-MIB in various water sources, as can be seen in Table 1.8.

The ozonation kinetics is also studied. In batch, ozonation of geosmin and 2-MIB is a second-order reaction (Westerhoff et al., 2006). While ozone was added continuously, it followed approximately a first-order reaction in other studies. However, the volatilization of the T&O compounds was not considered (Liang et al., 2007) or observed (Yuan et al., 2013) in those studies.

Furthermore, ozonation is also effective in degrading intracellular geosmin by damaging the cell and reacting with the released geosmin (Yuan et al., 2013). A higher dosage is required to achieve better geosmin removal.

While ozone is effective in removing these compounds, a high dosage is required for complete removal. However, a high ozone dosage may result in significant bromate formation (Yao et al., 2017). Therefore, UV light or H_2O_2 is added to reduce the O_3 dosage, as shown in Table 1.9.

The addition of H_2O_2 in ozonation efficiently degrades a low amount of geosmin and 2-MIB when the reaction was completed within 10 min (Mizuno et al., 2011; Park et al., 2006).

However, hydrogen peroxide may impair the disinfection effect of ozone. Moreover, H_2O_2 needs special care on storage and handling cause it's reactive and easy to decay. To

Table 1.8 Ozone treatment for geosmin and 2-MIB

Initial concentration ($C_{geosmin} = C_{2-MIB}$)	Matrix	O₃ dose (mg·L⁻¹)	Reaction condition	Removal efficiency		Ref
				Geosmin	2-MIB	
30 - 130 ng·L⁻¹	Nano pure water	0.75-4 (ozonized water)	30 min pH=5.7-8.1	97% ~ >99% $K_{O3,\ geosmin}$ (M⁻¹ s⁻¹) =7.5	93% ~ >99% $K_{O3,2-MIB}$ (M⁻¹ s⁻¹) = 1	(Westerhoff et al., 2006)
15 - 100 ng·L⁻¹	River & reservoir	3.75-5 (ozonized water)	20 min	95% ~ >99%	93% ~ >99%	
100 -500 ng·L⁻¹	Millli-Q water	4.19 (ozone-flotation)	20 min pH=5.4-9.1	88.5%-100%	47.1%-100%	(Yuan et al., 2013)
1623 ng·L⁻¹	Algal suspension	4.19 (ozone-flotation)	20 min pH=7.3	99.91%	-	
~10 µg·L⁻¹	Reservoir	O₃=1.175 – 5.875 mg·L⁻¹ (ozonized water)	pH=7.9-8.1, reaction time = 40 min	14% - 50%	7%-46%	(Yao et al., 2017)
15.0-52.1 ng·kg⁻¹ (2-MIB) 52.4-384.3 ng·kg⁻¹ (geosmin)	Fillet in RAS	(ozone-flotation)	0.25-0.28	no significant effect		(Schrader et al., 2010)
-	Fish muscle	3.3 mg· L⁻¹, 5.1 mg·L⁻¹, and 7.6 mg·L⁻¹ (ozonized water)	20 min	42.09%–54.28%	-	(Zhang et al., 2016)
		0.3 m³·h⁻¹ (ozone-flotation)	5-20 min	42.78%–69.19%	-	

Table 1.9 UV/O$_3$ and O$_3$/H$_2$O$_2$ treatment for geosmin and 2-MIB

Initial concentration (C$_{geosmin}$ =C$_{2\text{-MIB}}$)	Matrix	Reaction condition	Efficiency		Reference
			Geosmin	2-MIB	
50 / 100 ng·L^{-1} (only 2-MIB)	River & reservoir	O$_3$=3 mg·L^{-1} (ozonized water) 0.05 mg H$_2$O$_2$/ mg O$_3$		98%~99%	(Westerhoff et al., 2006)
~10 µg·L^{-1}	Reservoir	electro-generate H$_2$O$_2$, current = 20-40 mA, c(O$_3$) = 4.7 mg L^{-1}, reaction time =5 min	k=1.57 × 10^{-1} min^{-1} 50%-55%	k=1.21 × 10^{-1} min^{-1} 40%-50%	(Yao et al., 2017)
		electro-generate H$_2$O$_2$, current = 40 mA, c(O$_3$) = 3 mg L^{-1}, gas flow rate= 0.17 L min^{-1} reaction time =20 min	k=1.152 × 10^{-1} min^{-1} 90%	k=0.678 × 10^{-1} min^{-1} ~74%	
117 ng·L^{-1} (geosmin) 171 ng·L^{-1} (2-MIB)	Sand filtered water	O$_3$/H$_2$O$_2$, c(O$_3$) = 1-2 mg·L^{-1}, c(H$_2$O$_2$) = 0.15-0.6 mg·L^{-1} (add O$_3$ and mixed solution continuously)	k=1-1.8 × 10^{-3} s^{-1} 74-96% removal, in 1 min	k=0.9-1.8 ×10^{-3} s^{-1} 69%-95% removal in 1 min	(Park et al., 2007)
58-609 ng·L^{-1}	River	O$_3$/H$_2$O$_2$, c(O$_3$) = 2 mg·L^{-1}, c(H$_2$O$_2$) =3.7 mg·L^{-1} (add O$_3$ and mixed solution continuously)	1.3-14 ng·L^{-1} (10 min)	3.9-18 ng·L^{-1} (10 min)	(Mizuno et al., 2011)

solve this problem, an O_3/electro-peroxone (E-peroxone) process is applied. During this process, *in-situ* H_2O_2 is generated. The E-peroxone process occurred at a higher rate and lower bromate formation than conventional ozonation (Yao et al., 2017).

In a natural water treatment situation, a pilot study of O_3/GAC shows that the removal of geosmin and 2-MIB is efficient with a low dosage of ozone ($1mg·L^{-1}$) in combination with conventional treatment (flocculation, sedimentation, sand filtration, and GAC filtration) (Chen et al., 2019). However, due to the presence of NOM, additional treatment for regeneration of GAC is required (Chestnutt et al., 2007).

1.6.3   Photolysis

Photolysis reaction is also regarded as an efficient way to degrade resistant organics. The photolytic reaction of geosmin and 2-MIB is widely studied. These methods can be divided into two streams. Firstly, UV light is added in conventional treatment, including ozonation and hydrogen peroxide. The other part is the degradation of these two compounds with various photocatalysts with the illumination of UV.

UV light accelerates the generation rate of free radicals during reaction with ozone and hydrogen peroxide. Ozonation is enhanced in photolysis because H_2O_2 is produced as an intermediate, producing more HO· (Elkacmi & Bennajah, 2019; Zoschke et al., 2012).

$$O_3 + h\upsilon \rightarrow {}^1O_2 + O\ (^1D) \tag{11}$$

$$O\ (^1D) + H_2O\ (gas\ phase) \rightarrow 2HO· \tag{12}$$

$$O\ (^1D) + H_2O\ (liquid\ phase) \rightarrow H_2O_2 \tag{13}$$

$$H_2O_2 + 2O_3 \rightarrow 2O_2 + 2HO_2· \tag{14}$$

The mechanism associated with UV and H_2O_2 reaction is listed as following (Jo et al., 2011)

$$H_2O_2 + h\upsilon \rightarrow 2HO· \tag{15}$$

$$HO\cdot + \text{R-H} \rightarrow H_2O + R\cdot \tag{16}$$
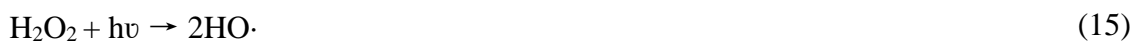
The following equations show the chain reaction involved in the UV/chlorine process (Feng et al., 2007)

$$Cl_2 + H_2O \rightarrow HOCl + HCl \tag{17}$$

$$HOCl + h\upsilon \rightarrow OH\cdot + Cl\cdot \tag{18}$$

$$OCl^- + h\upsilon \rightarrow \cdot O^- + Cl\cdot \tag{19}$$

$$\cdot O^- + H_2O \rightarrow \cdot OH + OH^- \tag{20}$$

$$OH\cdot + HOCl \rightarrow H_2O + \cdot OCl \tag{21}$$

$$OH\cdot + OCl^- \rightarrow OH^- + \cdot OCl \tag{22}$$
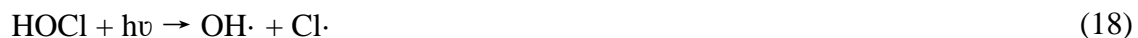
UV/H_2O_2 or UV/O_3, UV/chlorine can degrade geosmin and 2-MIB to values below their odor thresholds (Kim et al., 2016; Ma et al., 2018; Wang et al., 2015; Zoschke et al., 2012). The factors affecting these processes include water matrix, UV lamp power, optical path length, irradiated volume, and dosage of oxidants.

In raw water application, UV/O_3 is better than UV/H_2O_2 because, in raw water, the NOM acts as a scavenger for hydroxyl radicals. For UV/H_2O_2 and UV/O_3, though both can degrade more than 90%, the removal efficiency is lower in raw water than in pure water. The influence of NOM on UV/chlorine degrading geosmin and 2-MIB hasn't been reported.

On the other hand, the presence of NOM in raw water also accelerates the decomposition of ozone, so more hydroxyl radical is generated. Therefore, the efficiency of the UV/O_3 process is impaired less (Liang et al., 2007; Newcombe et al., 2002; Zoschke et al., 2012). However, too much NOM may lead to uneconomic circumstances. For instance, in recirculated aquaculture systems, the abundant impurities require a pre-treatment method (Klausen & Grønborg, 2010).

From the perspective of energy, UV/O$_3$ and UV/chlorine are superior to UV/H$_2$O$_2$ generally (Miklos et al., 2018). This is because Electrical Energy per order (E$_{EO}$) is calculated mainly based on UV illumination time (Zoschke et al., 2012). The UV/O$_3$ reaction is faster, so less UV illumination time is required compared to UV/H$_2$O$_2$. The comparison of E$_{EO}$ with different techniques is shown in Table 1.10.

Table 1.10 Electrical Energy per order (E$_{EO}$) comparison of UV based AOPs in raw water

Process	E$_{EO}$, geosmin (kWh m^3)	E$_{EO}$, 2-MIB (kWh m^3)	Reference
UV/O$_3$	0.5	0.5	(Zoschke et al., 2012)
VUV	1.3	1.4	
UV/H$_2$O$_2$	2.8	4	
UV/H$_2$O$_2$	1.32	1.32	(Rosenfeldt et al., 2005)
UV/H$_2$O$_2$	0.29-0.60	0.34-0.90	(Wang et al., 2015)
UV/Chlorine (pH=7.5)	0.28-0.49	0.34-0.68	

Another study shows that UV/chlorine is more economical than UV/H$_2$O$_2$ in full-scale tests (Wang et al., 2015). The superiority of UV/chlorine contributes to stronger medium pressure UV light absorption (HOCl and OCl$^-$ absorb UV light 2.3 and 10.7 times respectively more than H$_2$O$_2$) and similar hydroxyl production with H$_2$O$_2$ (Wang et al., 2012).

It's worth mentioning that though slower $\cdot$OH reaction with HOCl (8.46×10^4 M^{-1} s^{-1}, (Watts & Linden, 2007)) than H$_2$O$_2$ (2.7×10^7 M^{-1} s^{-1}, (Goldstein et al., 2007)) was considered as another reason (Wang et al., 2015), while the reaction of $\cdot$OH and $\cdot$OCl

dominates the termination reaction with higher rate constant (8×10^9 M^{-1} s^{-1}, (Watts & Linden, 2007)).

Moreover, another drawback of UV/H_2O_2 is the residual H_2O_2. Only a small amount of H_2O_2 is used during oxidation. So the residual H_2O_2 needs to be removed to meet the drinking water standard. (Zoschke et al., 2012).

1.6.4   Photocatalysis

During photocatalysis, free radicals are produced under UV or solar light in the presence of a catalyst. These catalysts are mainly semiconductor materials that can be excited under light and have electrons and valence band holes. The organic compounds are oxidized by valence band holes (positive charge) and reduced by electrons. The implementation of photocatalyst makes it possible to process wastewater in mild temperature and pressure conditions. Considering both chemical feasibility and economic constraints, TiO_2 is the best semiconductor with a low energy band gap (3.2eV) (Krzemińska et al., 2015). The mechanism of photocatalysis by TiO_2 is shown as the following equations.

$$TiO_2 + h\upsilon \rightarrow e^- + h^+ \tag{23}$$

$$e^- + O_2 \rightarrow O_2^- \cdot \tag{24}$$

$$h^+ + H_2O \rightarrow H^+ + HO \cdot \tag{25}$$

$$h^+ + OH^- \rightarrow HO \cdot \tag{26}$$

$$O_2^- \cdot + H^+ \rightarrow HO_2 \cdot \tag{27}$$

The photocatalytic reaction of geosmin and 2-MIB has been widely studied. Degussa P25 has the best removal efficiency for currently available catalysts after comparing commercially available catalysts (Degussa P25, Kronos vlp-7000) and home-prepared materials (N-TiO_2, GO–TiO_2, and Ref-TiO_2) under UV, solar and visible light. The results show that all these catalysts can degrade geosmin and 2-MIB under UV or solar light. Especially, the reaction time to complete the reaction using Degussa P25 is within

30 min, no matter with different light sources. The result indicates the potential to replace expensive UV light with Degussa P25 in a real application (Fotiou et al., 2015).

In the study above, to narrow the bandgap, some catalysts were derived by modifying TiO_2. This helps the catalysts enhance the photoresponse to visible light (Fotiou et al., 2015). Furthermore, another modified TiO_2 is studied, including Fe-N co-doped TiO_2 (Yuan et al., 2018) and $C\text{-}TiO_2$ (Fotiou et al., 2016). The removal efficiency of 2-MIB in 2 h is as following: $GO\text{-}TiO_2$ (100%) > Fe-N co-doped TiO_2 (90%) > $N\text{-}TiO_2$ (70%) > $C\text{-}TiO_2$ (0%). Moreover, catalysts based on other catalysts, including palladium (Pd) modified tungsten trioxide (WO_3), Zn-Al-LDH (Xue et al., 2016), are also efficient in degrading geosmin and 2-MIB.

A pathway study revealed the intermediates and by-products of photocatalytic reactions. The by-products after photocatalysis is harmless for human, but carcinogenic compounds may be produced if the process is combined with chlorine disinfection (Bamuza-Pemu & Chirwa, 2012).

However, the activity of TiO_2 may decrease because of impurities in water (Burns et al., 1999), so pre-treatment of water is necessary. Especially, TiO_2 based on graphene oxide shows resistance to complex water matrix (Cruz et al., 2017).

In the real application in water treatment, other than the influence of NOM, the existence high concentration of TiO_2 in water may threaten human health (Long et al., 2006; Xia et al., 2006). To separate the catalyst, various immobilization methods of catalyst are studied. For instance, sol-gel methods have been applied to immobilize the $TiO_2\text{-}SiO_2$ mixture on glass slides (Yaparatne et al., 2018). The spray coating method immobilizes TiO_2 on a glass plate and has been applied in RAS (Pettit et al., 2014; Zhao et al., 2015). Layer-by-layer dip-coating to immobilize titania (TiO_2) and Y zeolite composite show synergism of adsorption and photodegradation (Wee et al., 2015).

Furthermore, membranes are often applied to detain the catalyst. Conventional membrane filtration processes only concentrate pollutants and form a cake layer and result in pore blocking. Contrarily, photocatalyst can degrade pollutants. Hence photocatalytic

membrane reactor (PMR), which coupling photocatalysis with membrane separation can be applied (Zheng et al., 2017, Gupta et al., 2021). PMR has the advantage of saving energy and cutting down the installation size (Riaz & Park, 2020).

1.6.5   Fenton process

Ferrous iron reacts as a catalyst, and it can be regenerated.

$$Fe^{2+} + H_2O_2 \rightarrow Fe^{3+} + OH^- + OH\cdot \tag{28}$$

$$Fe^{3+} + H_2O_2 \rightarrow Fe^{2+} + HO_2\cdot + H^+ \tag{29}$$

$$Fe^{3+} + HO_2\cdot \rightarrow Fe^{2+} + O_2 + H^+ \tag{30}$$

With illumination, the regeneration rate of Fe (II) accelerates, leading to the production of more radicals (Khataee et al., 2014).

$$Fe(OH)^{2+} + h\upsilon \rightarrow Fe^{2+} + OH\cdot \tag{31}$$

$$Fe(RCO_2)^{2+} + h\upsilon \rightarrow Fe^{2+} + CO_2 + \cdot R \tag{32}$$

$$H_2O_2 + h\upsilon \rightarrow 2OH\cdot \tag{33}$$
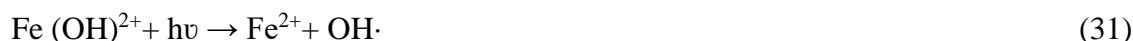
However, H_2O_2 is difficult to transport, store and handling and ferrous ion needs a stable supply (Díez et al., 2016). Therefore, besides adding regent, electrochemical reactions can be a continuous source of H_2O_2 and Fe^{2+}. It is achieved by oxidizing Fe anode or reducing ferric iron.

$$O_2 + 2H^+ + 2e\text{-} \rightarrow H_2O_2 \tag{34}$$

$$Fe^{3+} + e\text{-} \rightarrow Fe^{2+} \tag{35}$$

$$Fe \rightarrow Fe^{2+} + 2e^- \tag{36}$$

Factors that influence this process include pH, number of ferrous ions, initial concentration of H_2O_2, and the pollutant and presence of other ions. It has the advantage of high mineralization by degrading both organic and inorganic contaminants. Moreover,

the cost is relatively low because of easy operation and the high removal rate (Krzemińska et al., 2015).

There are two forms of Fenton catalysts. The homogeneous solution has higher efficiency in oxidizing, but an extra process is needed to remove abundant catalysts (Ormad et al., 2006). In contrast, the heterogeneous Fenton process is easy to separate excess solid iron in solution (Mosteo et al., 2006). Still, the efficiency is lower because of light scattering effects in suspended iron particles inhibiting the light efficiency, and mass transfer is restricted in the heterogeneous matrix (Ioannou et al., 2013).

The application of photo-Fenton in degradation of geosmin and 2-MIB revealed the best removal at pH=3. The addition of H_2O_2 can facilitate the removal efficiency, and it is reduced in the presence of NOM, higher pH, and initial concentration of geosmin and 2-MIB (Park et al., 2017).

1.6.6   Ferrate

Potassium ferrate is considered an environmentally friendly oxidant in water treatment. It is a powerful oxidizing agent in a wide pH range and produces non-toxic by-product Fe (III) or ferric hydroxide, a coagulant (Jiang & Lloyd, 2002; Sharma, 2002).

However, ferrate shows low degradation efficiency of geosmin and 2-MIB. The best degradation rate of 25% is observed using ferrate alone (Feng et al., 2017; Park et al., 2007). This is much lower than other AOP methods based on hydroxyl radicals. The inefficiency results from the selectivity of Fe (VI).

1.6.7   Wet Air Oxidation (WAO)

Wet Air Oxidation (WAO) is a process operating at high temperatures (125 to 320 °C), high pressure (200 bar), and low pH. The extreme condition ensures reaction between organic compounds in an aqueous solution with oxygen. This method has the advantage of higher COD removal efficiency and harmless products such as CO_2, H_2O (Elkacmi & Bennajah, 2019).

However, the severe operating condition results in a high cost of WAO. Hence, the addition of catalysts in WAO is known as catalytic wet air oxidation (CWAO). CWAO operates in milder conditions requiring less energy. Heterogeneous catalysts are superior to homogeneous ones due to lower separation costs. Noble metal catalysts perform better in degradation, but they are unstable and expensive. Alternatively, non-noble metal catalysts with support is a promising catalytic system (Sushma et al., 2018).

Nevertheless, the application of WAO for the removal of geosmin and MIB has not been studied.

1.6.8   Ultrasonic irradiation

Ultrasound leads to the formation and growth of unstable cavities due to the collapse of air bubbles in the water. The immediate destruction of cavities releases energy that is capable of dissociating H_2O into hydroxyl radicals. Hence the generated OH· reacts with pollutants.

Ultrasonication of geosmin and 2-MIB was tested by Nam-Kon et al. (2016), Song and Shea (2007). The ultrasonication process exhibits apparent first-order kinetics with a rate constant of 0.07 and 0.12 min^{-1} for 2-MIB and geosmin, respectively. It reveals that the hydrolysis induced by cavitation dominants the reaction. Moreover, to enhance this process, high-frequency ultrasound and increasing salinity can be applied. Compared with GAC absorption or photocatalysis, ultrasonic irradiation is more resistant to (in)organic load. However, ultrasonic equipment is costly in large-scale treatment. (Nam-Koong et al., 2016; Song & O'Shea, 2007)

1.6.9   SR-AOPs

As an alternative for hydroxyl radical-based AOPs, sulfate radical-based AOPs (SR-AOPs) have drawn attention recently. For oxidant strength, the redox potential of $\cdot SO_4$ (E^0=2.6V) is competitive with $\cdot OH$ (E^0=2.8V) though slightly lower (Oh et al., 2016). However, $\cdot SO_4$ possesses reactivity for a longer lifetime ($t_{1/2, \cdot SO4}$ =30-40 μs vs. $t_{1/2, \cdot OH}$ = 10^{-3} μs) (Olmez-Hanci & Arslan-Alaton, 2013) and higher quantum yield (He et al., 2013).

For practical application, hydroxyl reacts readily with scavengers, including natural organic matter (NOM) and alkalinity. The non-selectivity of hydroxyl results in less effectivity in pollutant removal requiring higher dosage (He et al., 2013; Oh et al., 2016)

On the contrary, sulfate radicals react selectively with electron-donating groups. This feature eliminates the influence of the water matrix (Oh et al., 2016). Furthermore, the transition metals in the water matrix accelerate the reactivity of sulfate radicals (He et al., 2013). Moreover, PMS costs are lower for storage and transportation than H_2O_2 (Ling et al., 2010).

As common sources for sulfate radical, peroxymonosulfate (PMS) and persulfate (PS) need to be activated. There are mainly two methods to active PMS and PS. The first one is to add energy such as heat, ultrasound, or UV light. However, the high capital cost hinders the application of this method.

Alternatively, catalysts are widely studied for economic reasons. Catalysts based on transition metal (Co, Cu, Fe, Mn) and nonmetal catalysts have proved efficient as the activator (Oh et al., 2016). Iron-based activators have the advantage of being environmentally friendly from a sustainability perspective (Feng et al., 2017).

In summary, the removal of geosmin and 2-MIB from water has been widely studied. Previous studies show the absorption can be affected by NOM easily. Microbial treatment can remove the T&O compounds, but the long reaction time restricts the application in occasionally occurred algae bloom-caused smell. AOPs are efficient in removal, while the utilization of UV light increases the capital cost. Furthermore, the pathway analysis also shows photocatalysis may produce toxic by-products in combination with chlorine treatment.

Chapter 2

2.   Detection of geosmin and 2-methylisoborneol by dispersive liquid-liquid micro-extraction flame ionization detection (DLLME-FID)

2.1   Background

Dispersive liquid-liquid micro-extraction (DLLME) is a sample preparation technique based on the different affinities of analytes to sample and extractant, which is similar to liquid-liquid extraction. Due to the small amount of extractant, DLLME has an advantage in environmentally friendly, economical, simple operation, and rapid separation (Ahmad et al., 2015).

The procedure of DLLME is shown in Fig 2.1. Extractant and dispersive solvents are added into an aqueous solution sample. Then a cloudy solution, made up of the microdroplets of extraction solvent, is formed by physical phase disruption such as rapid injection, shaking, or ultrasound (Ahmad et al., 2015; Quigley et al., 2016). The microdroplets are distributed uniformly in aqueous samples through a disperser. The microdroplets increase the surface area that achieves rapid mass transfer between sample solution and extractant (Ahmad et al., 2015). Then the sedimented phase is collected after centrifugation for analysis.

To obtain high extract efficiency, proper selection of dispersive solvent and extractant is crucial for DLLME. The disperser needs to be soluble with both the water phase and extractant. In contrast, the solubility of extractants needs to be high in disperser while low in the water. To separate different phases, the density of extractant and water must be distinguishable (Zgoła-Grześkowiak & Grześkowiak, 2011).
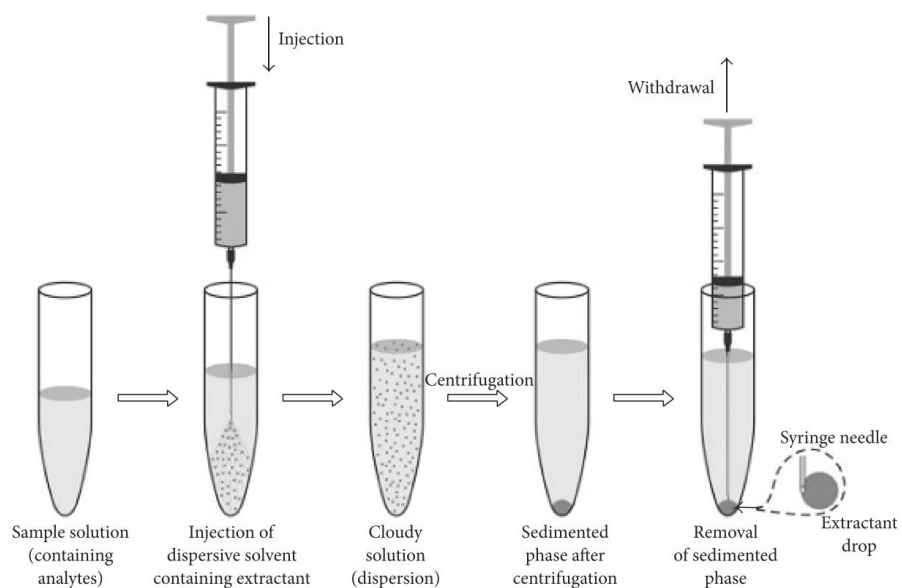
Figure 2.1 Schematic of DLLME technique (Zgoła-Grześkowiak & Grześkowiak, 2011)

If the density of the extractant is higher than water, the sedimented extraction solvent can be collected by syringe. However, if the extractant floated on top of the water, specialized glassware can trap the solvent as shown in Figure 2.2. (Farajzadeh & Mogaddam, 2012). Alternatively, a simpler process to separate the floating extractant drop is to freeze the vessel and collect the frozen drop. However, this frozen process is only useful for solvents with melting points close to room temperature (Melwanki & Fuh, 2008; Kocúrová et al., 2012).
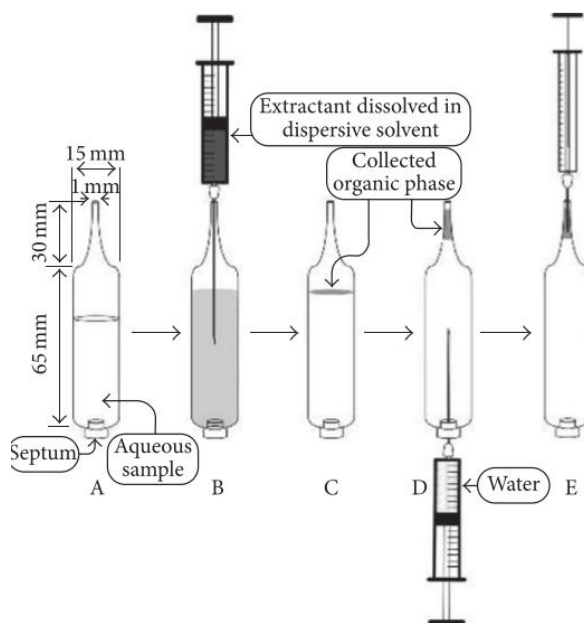
Figure 2.2 low-density solvent-based DLLME (LDS-DLLME) using specialized glassware

Two studies were performed for the analysis of geosmin and 2-MIB by DLLME. Firstly, ultrasound was applied to assist the dispersion of the DLLME procedure (Cortada et al., 2011). Parameters influencing DLLME were optimized, including solvent and sample volume, solvent type, centrifugation speed, extraction time, and temperature. This process can analyze geosmin and 2-MIB with limits of detection of 2 and 9 ng·L^{-1}, respectively. However, ultrasound can degrade around 30% of geosmin and 2-MIB at low frequency (20 kHz) (Nam-Koong et al., 2016). It means this method may impair the analytes.

In another study (Tian et al., 2017), ultrasound was replaced by shaking manually. Additionally, the mixed solution needs to be frozen and thawed for phase separation. Different combinations of dispersants and extraction solvents were studied. This methodology achieves good linearity in the range of 5-100 µg·L^{-1}. However, the limit of quantitation (LOQ) is higher than the previous study. LOQ of geosmin and 2-MIB is 100 and 150 ng·L^{-1}, respectively.

Considering the simplicity of operation and high efficiency, DLLME is applied in this study. In addition, the reaction time was shortened from > 30 min to less than < 10 min without freezing and thawing. In this work, the analysis protocol of Tian et al., (2017) was adopted.

2.2   Materials and experimental methods

2.2.1   Chemicals

The gas chromatography standard of GSM and 2- MIB was purchased from Sigma-Aldrich at a 100 μg·L^{-1} concentration. The mixture sample was prepared in Milli-Q water at a concentration of 100 μg·L^{-1}. The internal standard 1-chlorooctane was purchased from Sigma-Aldrich and dissolved in acetone (0.16 g·L^{-1}). Chloroform and acetonitrile were high-performance liquid chromatography (HPLC) grade purchased from Sigma-Aldrich.

2.2.2   Instrumentation

The samples were injected by Agilent 7693A automatic liquid sampler and analyzed in a gas chromatograph with flame ionization detector (GC-FID; Agilent 7890A; Agilent Technologies, Mississauga, ON, Canada) with an HP-5ms column (30 m × 320 μm x 0.25 μm; Agilent Technologies, Mississauga, ON, Canada). The specific analysis conditions are as follows. The oven temperature program was held at 60 ℃ for 4 min, raised to 280 ℃ at increments of 12℃ min^{-1}. The carrier gas was ultra-pure helium (99.9999%) and was kept at 1 mL·min^{-1} constant flow rate. The injection port was set at 250°C in spitless mode, and the injection volume was 1μL.

2.2.3   Procedure

10 mL sample was added into a 15 mL glass test tube with conical bottom. 400 μL of acetonitrile and 100 μL of chloroform were added at the same time. 10 μL internal standard was added. Then the tube was shaken vigorously by hand for 3 min. Afterward, the mixed solution was centrifuged at 2300 rpm for 2 min. The enriched analytes in the chloroform were transferred to auto sampling vials with 0.05 mL inserts followed by injection into GC-FID.

2.2.4   Results and discussion

2.2.4.1   Recoveries of dispersive liquid-liquid micro-extraction

2-MIB and GSM mixed solution were spiked in Milli-Q water, and the DLLME extraction results are shown in Table 2.1.

Table 2.1 Recoveries of 2-MIB and geosmin spiked in pure water at different concentrations (n = 3)

Concentration/($\mu g \cdot L^{-1}$)	MIB		GSM	
	Recovery/%	RSD/%	Recovery/%	RSD/%
10	115	1.2	108	2.0
30	104	1.1	100	0.6
60	98	7.9	98	9.0
100	92	0.3	94	2.2
200	102	2.0	100	3.2

Good recoveries and relative standard deviations were obtained. The recoveries obtained from different concentrations are slightly different. For 2-MIB, the recovery ranges from 92 % to 115 %, while the recoveries of GSM perform better, which ranges from 94 % to 108 %. The results revealed that DLLME is efficient for the analysis of 2-MIB and GSM.

2.2.4.2   Linear ranges and detection limits

2-MIB and GSM mixed samples at a concentration between 3-200 $\mu g \cdot L^{-1}$ were extracted by the DLLME method to draw calibration curves. The limitations of quantification were determined by injecting a series of low concentration solvents to produce a signal-to-noise ratio (S/N) of 10. Then the original concentrations were calculated as the limits of quantitation for 2-MIB and GSM. Details are shown in Table 2.2. Y stands for the peak area ratio of target compounds and internal standard compound, while X stands for the peak area ratio of target compounds with internal standard.

Table 2.2 The equations, linear ranges, correlation coefficients and limit of quantitations (LOQs) of the method

Compounds	Calibration curve	Range/ ($\mu g \cdot L^{-1}$)	LOD[1]	LOQ[2]	R^2
2-MIB	Y=0.00601X+0.01043	3-200	0.16	1	0.99267
GSM	Y=0.00596X+0.00636	3-200	0.16	1	0.99353

[1] Signal to noise =3.6

[2] Signal to noise =11.9 (MIB); 8.8 (GSM)

Chapter 3

3. Geosmin and 2-MIB treatment in water by ozonation

3.1 Introduction

Ozonation of geosmin in both batch and semi-batch modes was studied. To enhance the removal efficiency in batch, H_2O_2 was added to study the influence of H_2O_2 and O_3 dosage and pH.

To simulate a real water treatment situation, semi-batch tests were conducted. During this process, ozone is sparged continuously into a reactor with a fixed amount of geosmin. In semi-batch, we studied 1) the volatilization of geosmin; 2) the influence of pH (5.0,7.0, 9.0); 3) the effectivity of hydroxyl radical, which was proved by adding methanol as a scavenger. Then the kinetics of all these three processes were investigated.

3.2 Ozonation

A series of experiments were performed to determine the effect of pH and H_2O_2 on the ozonation of GSM and 2-MIB. The ozone concentration in Milli-Q water by sparging O_3 at different pH was studied to determine the ozone dosage.

In ozonation treatment, ozone was added in two ways. At first, ozonated water was applied for batch reaction with varying ozone concentrations at pH =5.0,7.0, and 9.0 and in the presence of H_2O_2.

In semi-batch tests, the kinetics of geosmin removal at different pH by sparging O_3 were determined. To determine the influence of aeration by sparging, volatilization tests were conducted. In addition, to investigate the scavenging effect of methanol in AOP, GSM and 2-MIB dissolved in different concentrations of methanol were studied.

3.2.1   Chemicals

In this experiment, potassium indigotrisulfonate was purchased from Acros Organics (New Jersey, USA). All chemicals such as sodium phosphate dibasic and sodium phosphate monobasic were analytical grade and used without any treatment.

3.2.2   Experimental procedure
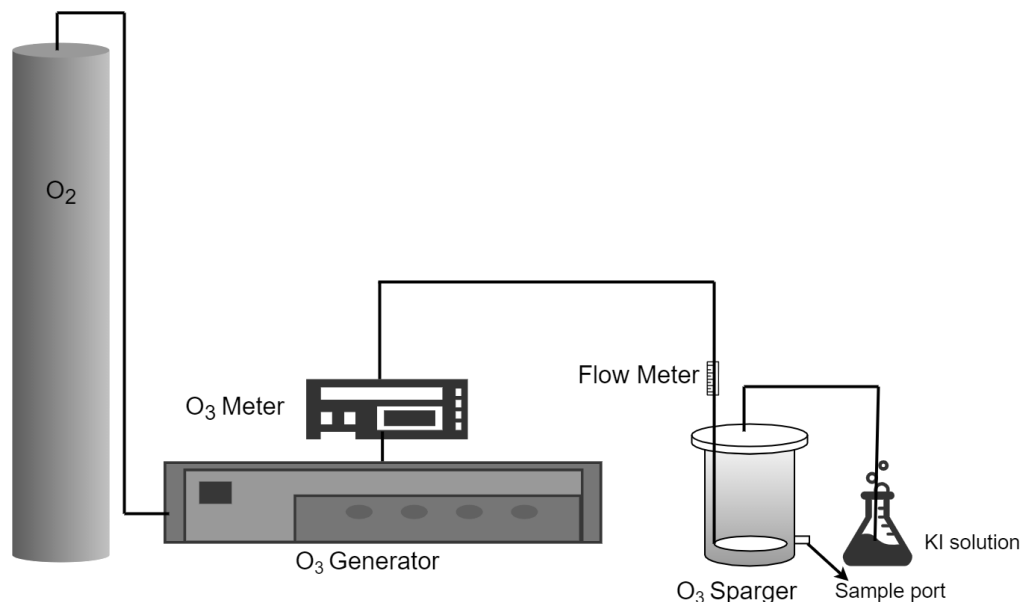
Figure 3.1 Schematic diagram of semi-batch ozonation reactor

3.2.2.1   Ozone concentration at different pH

Ozonation experiments were performed in a bench-scale batch reactor, as shown in Fig.3.1. Ozone was produced by an ozone generator (model TG-40, Ozone Solution, Hull, IA, USA) using compressed oxygen (ultra-pure) at a pressure of 10 psi. During an experiment, 500 mL solution at different pH was added into the batch reactor. Ozone was bubbled continuously in the reactor through a round shape diffuser (inner diameter 8.9 cm with 9 small holes) located at the bottom of the reactor. Ozone in the gas phase was measured using an ozone analyzer (model UV-100, Eco Sensors, Newark, California, USA). The ozone flow rate in the reactor was 4 L·min^{-1}, with a gas phase concentration around 2000 ppm. Samples of 10 ml were collected from the sample port. The solution

pH was adjusted by 50 mM phosphate buffer. All experiments were conducted in triplicate.

3.2.2.2   Ozonation of GSM and 2-MIB in batch

Effect of pH, H_2O_2, and O_3 concentration

Ozonated water was prepared by sparging ozone into the water with different pH values for 20 min. The O_3 concentration varies because of self-decomposition, which occurs fast from a few seconds to 1 or 2 min (Park et al., 2007). This phase is called instantaneous O_3 demand (ID). ID was measured every time. Then the solution was divided into Erlenmeyer flasks, each of them containing 40 mL ozonated water. Then geosmin and H_2O_2 solutions were added at the same time. The initial geosmin concentration was 20 $\mu g \cdot L^{-1}$ and H_2O_2 concentrations of 0, 0.138 $mg \cdot L^{-1}$, 0.2775 $mg \cdot L^{-1}$, 0.555 $mg \cdot L^{-1}$ and 1.1 $mg \cdot L^{-1}$ were studied. Samples were collected after 1 min and 10 min. The collected samples were quenched by adding 10 μL of saturated sodium thiosulfate immediately.

Kinetics

Ozonated water of different pH was obtained as before. The ozonated water was divided into 3 Erlenmeyer flasks, each of them containing 80 mL ozonated water. The ozone concentration was analyzed every time after dividing the solutions. Geosmin was added, and about 20 $\mu g \cdot L^{-1}$ and 0.2 $mg \cdot L^{-1} H_2O_2$ were spiked into the solution simultaneously.

3.2.2.3   Ozonation of GSM and 2-MIB by continuously sparging

Volatilization

250 mL of 20 $\mu g \cdot L^{-1}$ geosmin solution prepared in milli-Q water was added to the reactor. Then the ozone generator was turned off, and only oxygen was sparged into the stock solution. Samples were collected to determine the volatilization rate. The experiment was conducted in duplicate.

pH and Methanol scavenging effect

Stock solutions with 49 µM·L^{-1} and 1.49 µM·L^{-1} methanol with different pH were prepared in Milli-Q water. Then the solutions were added into the semi-batch reactor, and the ozone concentration in the gas phase was controlled at 2000 ppm. The reaction time was 40 min and 10 min for a different amount of methanol, respectively. The collected samples were quenched by adding 10 µL of saturated sodium thiosulfate immediately. All experiments were conducted in triplicates.

3.2.3   Analytical methods

Ozone concentration in Milli-Q water was measured by using decolorization of potassium indigotrisulfonate as described by Bader and Hoigné (Bader & Hoigne, 1982). The sulfonated indigo molecule contains only one C=C double bond, which reacts with one mole of O$_3$ and decolorizes indigo. The absorbance of the decolorized indigo solution was measured using a UV-Vis spectrophotometer (Model-Cary 60; Agilent technologies, CA, USA).

The concentrations of GSM and 2-MIB were analyzed by the DLLME method.

3.3   Results and discussion

3.3.1   Ozone concentration at different pH

The value of dissolved ozone concentration at different pH levels measured from a reaction time of 0 to 60 minutes is shown in Fig 3.2. It shows that dissolved ozone concentrations increase with increasing ozone time. However, after 15 minutes of ozonation, the dissolved ozone concentration was near to a constant value. Since the high mass transfer efficiency of ozone dissolving into water, ozone is saturated in water within seconds (Park et al., 2007). However, due to the poor performance, it took about 15 min to stabilize. Therefore, ozonated water was collected after 15 min. Moreover, the error bar shows inconsistent performance, which requires analyzing ozone concentration every time.

The results also indicate that the highest ozone concentration was achieved at a pH of 7.0. When the pH is high (Beltran, 2003), the alkali condition will initiate and accelerate ozone decomposition.

$$O_3 + OH^- \rightarrow HO_2^- + O_2 \qquad\qquad k = 1.1 \times 10^8 \ dm^3 \ mol^{-1} \ s^{-1} \qquad\qquad (37)$$

$$O_3 + HO_2^- \rightarrow HO_2\cdot + O_3^{-}\cdot \qquad\qquad k < 10^4 \ dm^3 \ mol^{-1} \ s^{-1} \qquad\qquad (38)$$
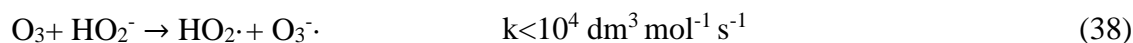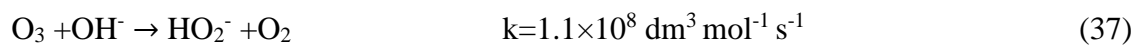
When the pH is lower (Sehested et al., 1991), $HO_2\cdot$ accumulates due to equation (39) and the slow reaction rate of equation (38). The increasing $HO_2\cdot$ terminate the reaction as equation (42). Therefore, the ozone concentration at pH=5.0 is lower as ozone is decomposed.
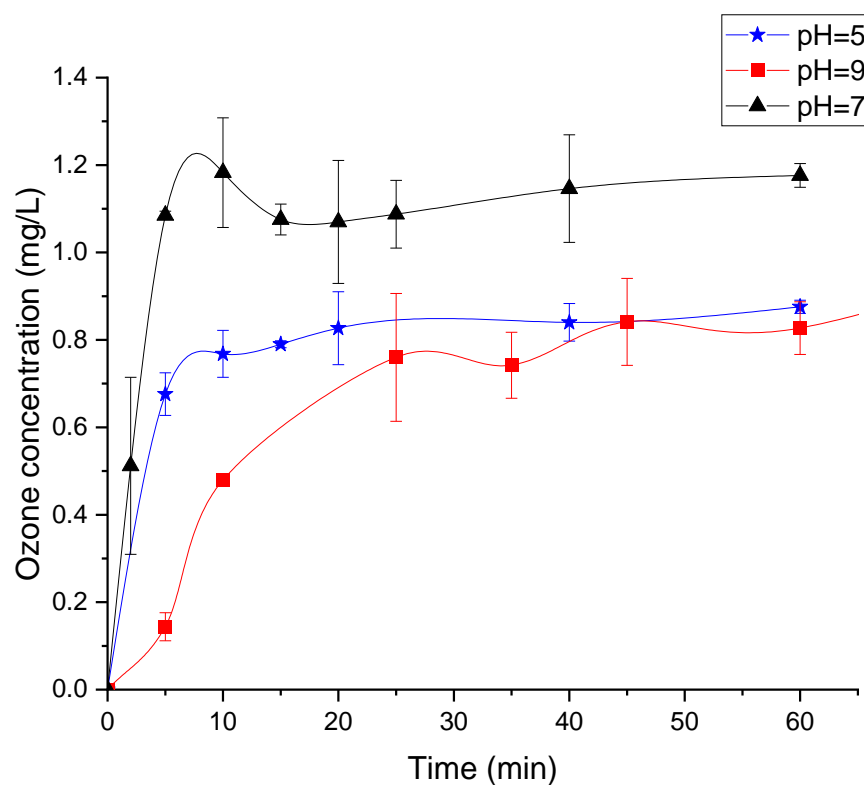
Figure 3.2 Effect of pH on dissolved ozone concentration in semi-batch. pH=5.0 (blue), pH=7.0 (black), pH=9.0 (red). Error bars indicate the standard deviation of the mean of three independent experiments

$$HO_2\cdot \leftrightarrow O_2^- + H^+ \qquad\qquad pK = 4.8 \qquad\qquad (39)$$

$$O_2^- + O_3 \rightarrow O_3^- + O_2 \qquad\qquad k = 1.5 \times 10^9 \ dm^3 \ mol^{-1} \ s^{-1} \qquad\qquad (40)$$

$$O_3^- + H^+ \rightarrow OH\cdot + O_2 \qquad\qquad k = 9 \times 10^9 \text{ dm}^3 \text{ mol}^{-1} \text{ s}^{-1} \qquad\qquad (41)$$

$$OH \cdot + HO_2 \cdot \rightarrow H_2O + O_2 \qquad\qquad k = 0.7 \times 10^{10} \text{ dm}^3 \text{ mol}^{-1} \text{ s}^{-1} \qquad\qquad (42)$$
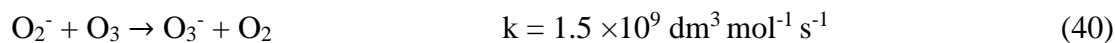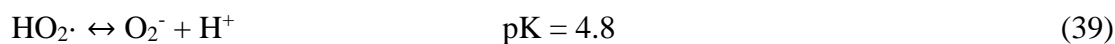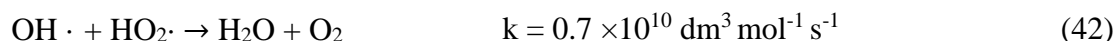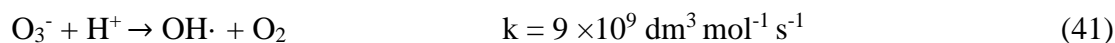
3.3.2 Geosmin removal in batch

pH, H_2O_2, and O_3 concentration

The O_3 concentration after ID was measured and is shown in the bracket at the x-axis in Figure 3.3. The number varies because of different pH (Ershov & Morozov, 2009) and operation time changes.

The influence of pH and H_2O_2/O_3 ratio is shown in Fig. 3.3.
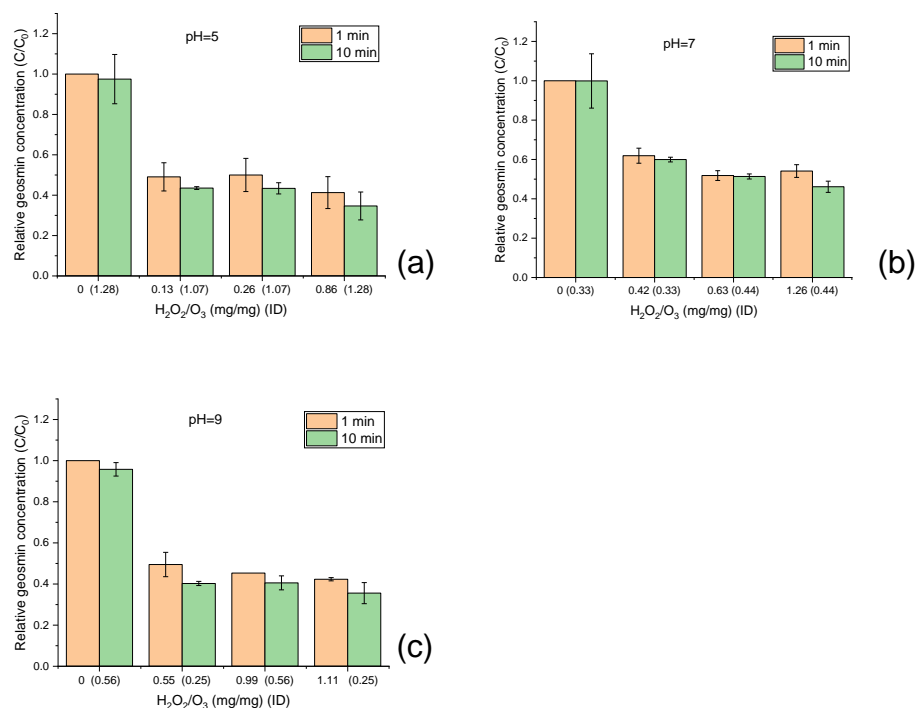
Figure 3.3 Geosmin degradation in batch by H_2O_2/O_3 at pH=5.0 (a); pH=7.0(b); pH=9.0(c). Samples were collected at 1 min (orange) and 10 min (green). (Geosmin initial concentration=20 µg·L^{-1}, instantaneous ozone demand (ID) is shown in the

brackets in x-axis.) Error bars indicate the standard deviation of the mean of three independent experiments

The extended reaction time only moderately contributed to the removal efficiency. The reaction removed about 50% of geosmin in 1 min. Only a little more geosmin is removed after 10 min. It indicts the high efficiency of H_2O_2/O_3 treatment. The fast degradation in 1 min is consistent with the previous study (Park et al., 2007). However, the total removal efficiency was lower than the study above as the ozonated water was added in batch rather than continuously; higher initial geosmin concentration may also be another reason.
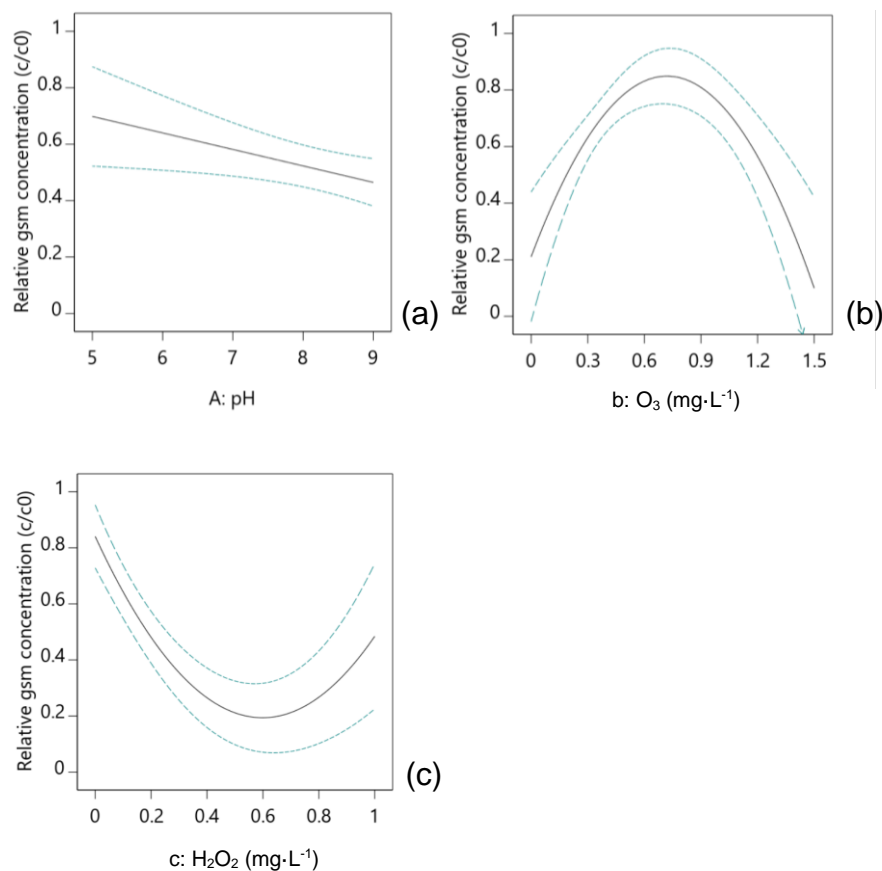
Figure 3.4 The influence of pH and H₂O₂ and O₃ dosage on geosmin degradation (These figures are based on regression analysis by Design Expert 11. The black lines

indicate the fitting curve and the blue lines indicate the 95% confidence interval bands)

The addition of H_2O_2 increased the removal of geosmin as H_2O_2 accelerates the decomposition of ozone. When ID is the same, the removal efficiency only increases slightly with the increasing H_2O_2/O_3. It may be because of insufficient supply of ozone. It is also possible that excessive H_2O_2 concentration may lead to scavenging of OH· (Jo et al., 2008).

At pH=9.0, low O_3 dosage achieved more geosmin removal. It means the higher ratio of H_2O_2/O_3 is more critical than the O_3 dosage in an alkaline environment.

To analyze the separate effect of factors including pH, O_3, and H_2O_2 concentration, Fig 3.4 were generated by software Design Expert 11 to discern the multivariate effects. The R^2 for the result is 0.8766.

Fig.3.4 (a) shows that the geosmin removal increases with the increase of pH. Fig.3.4 (b) shows the effect of adding H_2O_2 decreases if H_2O_2 is excessive. This may be because of the scavenging of OH· radical by H_2O_2. Fig.3.4(c) shows that the effect of O_3 can be divided into two parts. Before the vertex, extra O_3 isn't necessary for geosmin removal. It can be seen from Fig.3.2 that though the ozone concentration at pH=9 is lower than that of pH=5 or 7, the removal efficiency is similar at various pH (Fig.3.3). This is because radicals degrade the pollutants while O_3 decompose faster at an alkaline solution, generating more radicals (Ershov & Morozov, 2009).

3.3.3   Kinetics of geosmin removal by ozone/H_2O_2

The reaction condition is shown in Table 3.1. Fig. 3.5 shows the geosmin degradation over 30 min. In a previous study (Park et al., 2006), rate constants were calculated after the fast degradation period with a continuous supply of geosmin and ozone. However, it's not applicable here since the chemicals were consumed in 1 minute. The higher removal efficiency at pH=7 compared with pH=5 and 9 may cause by the high ozone concentration.
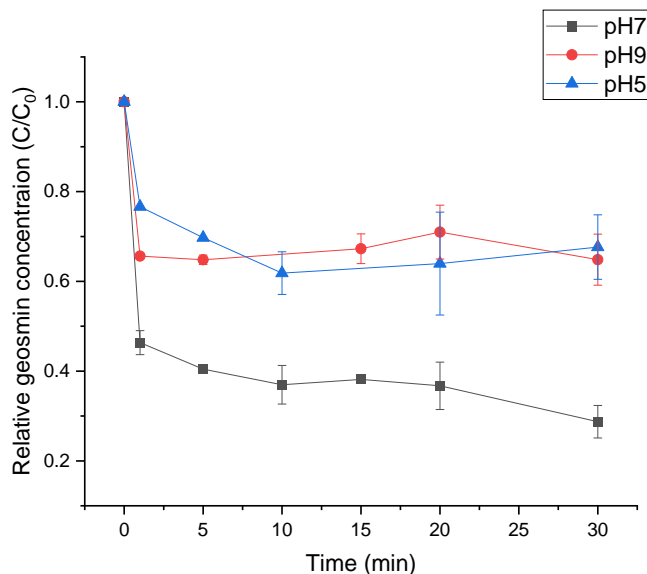
Figure 3.5 Kinetics study of 20 μg·L^{-1} Geosmin removal by ozone/H$_2$O$_2$ in batch at pH=5(blue), pH=7(black), pH=9(red). Error bars indicate the standard deviation of the mean of three independent experiments

**Table 3.1 Reaction parameters of kinetics study of geosmin degradation in batch by H$_2$O$_2$/O$_3$**

pH	5	7	9
H$_2$O$_2$/O$_3$ (mg/mg)	0.303	0.303	0.645
ID (mg·L^{-1})	0.66	0.66	0.31

3.3.4   Ozonation of GSM and 2-MIB by continuously sparging

The removal of geosmin and 2-MIB by semi-batch ozonation with continuous sparging of O$_2$/O$_3$ gas was investigated, to simulate real ozone reactors,

3.3.4.1   Volatilization of compounds

Since geosmin is volatile, only 75% is left after 10 min of continuous sparging (Fig.3.6a). It means that the geosmin loss during the aeration of ozone is not negligible. To compare

the volatilization kinetics with ozonation kinetics, later on, it is regarded as a pseudo-first reaction, and kinetic constants were determined via linear regression (inserted).
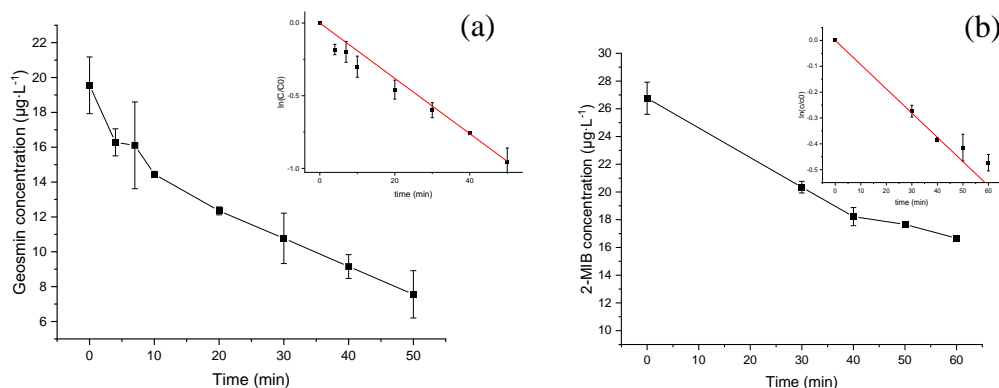
Figure 3.6 Geosmin(a) and 2-MIB(b) volatilization by sparging O_2 (n=2). The volatilization kinetics are shown in the inserted plots. Error bars indicate the standard deviation of the mean of two independent experiments

3.3.5   Continuous O_2/O_3 gas sparging

The ozone concentration in the gas phase is controlled as constant (flow rate of 4 L·min^{-1} with 2000 ppm O_3 in the gas phase). Assuming NTP, the concentration is calculated as equation (43):

$$C_{O3} = 4 \text{ L min}^{-1} / 24.2 \text{ L mol}^{-1} \times 2000 \text{ ppm} \times 10^{-6} \times 48 \text{ g mol}^{-1} = 0.016 \text{ g·min}^{-1} \qquad (43)$$

The comparison of Fig.3.7 and Fig.3.3 shows the removal efficiency in the semi-batch reactor is higher than that of the batch reactor without adding H_2O_2 generally. The removal efficiency follows pH9>pH7>pH5. It is consistent with the previous study (Liang et al., 2007). The increasing efficiency with pH is due to the self-decomposition of ozone-producing more hydroxyl radicals.

To prove the influence of hydroxy radical, scavenging tests were conducted. Because methanol acts as a scavenger for radicals, the addition of methanol should decrease the removal efficiency. The concentration of methanol in solution varies according to the different original concentrations of geosmin in solution. Fig. 3.7 and 3.8 show the
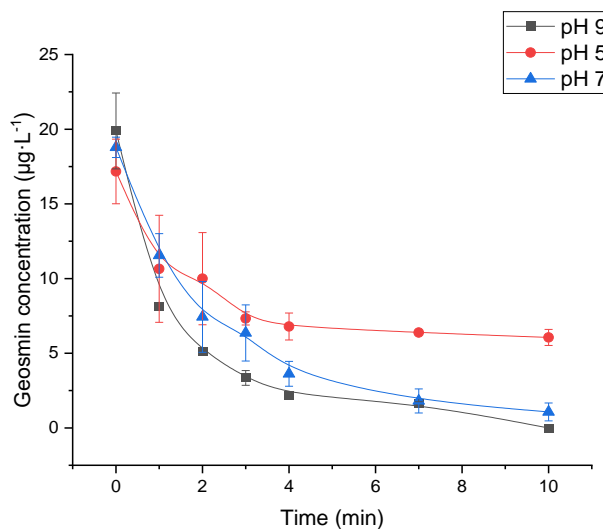
Figure 3.7 Geosmin removal in semi-batch at pH=5.0 (red), pH=7.0 (blue), pH=9.0 (black). (Methanol concentration = 1.48 μM·L^{-1}) Error bars indicate the standard deviation of the mean of three independent experiments
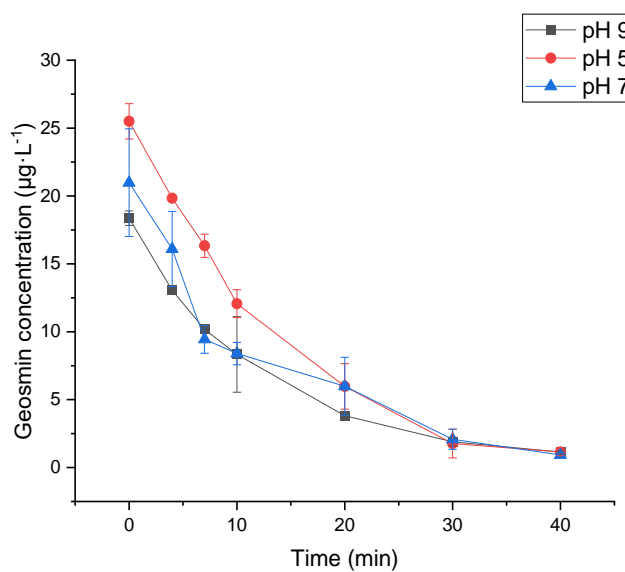
Figure 3.8 Geosmin removal in semi-batch at pH=5.0 (red), pH=7.0 (blue), pH=9.0 (black). (Methanol initial concentration = 49 μM·L^{-1}). Error bars indicate the standard deviation of the mean of three independent experiments
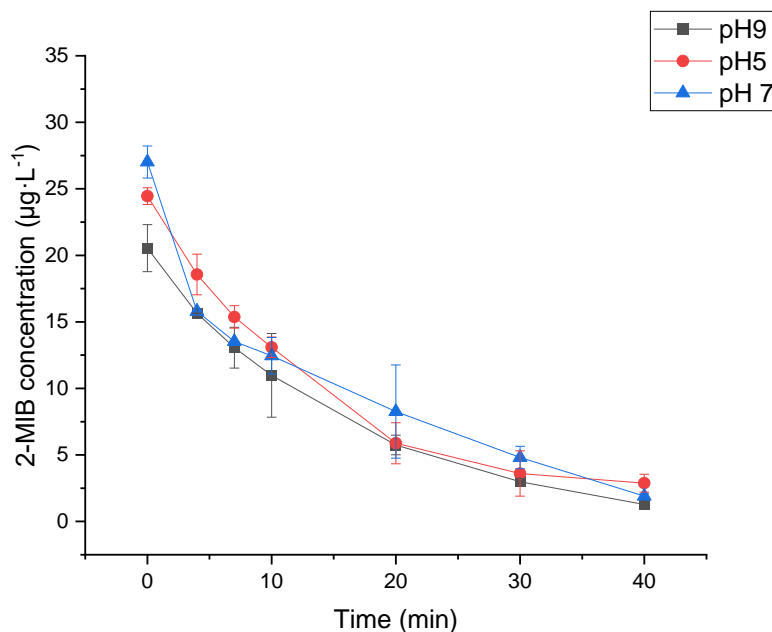
Figure 3.9 2-MIB removal in semi-batch at pH=5.0 (red), pH=7.0 (blue), pH=9.0 (black). (Methanol initial concentration=49 μM·L^{-1}) Error bars indicate the standard deviation of the mean of three independent experiments

reaction with less methanol takes less time (10 min vs. 40min), which means the radicals were quenched by methanol.

The results also imply that the ozone concentration is not the determined factor in the ozone process but the concentration of OH·. Fig.3.2 shows that at pH=9, the ozone concentration is lowest during sparging, while the geosmin removal is more efficient.

3.3.6   Kinetics

Assuming the removal process is first-order reaction, the reaction follows these linear equations:

$$\ln\left(\frac{C_{2-MIB}}{C_{02-MIB}}\right) = -k_1 t \tag{44}$$

$$\ln\left(\frac{C_{geosmin}}{C_{geosmin}}\right) = -k_2 t \tag{45}$$
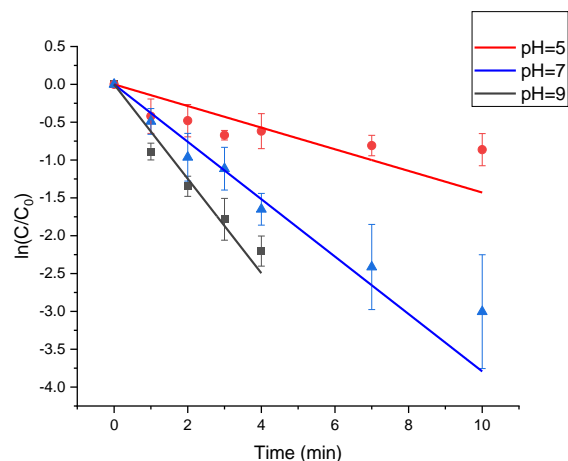
Figure 3.10 Geosmin removal kinetics in semi-batch at pH=5.0 (red), pH=7.0 (blue), pH=9.0 (black). (Methanol initial concentration=1.48 μM·L^{-1}, geosmin initial concentration≈20 μg·L^{-1}). Error bars indicate the standard deviation of the mean of three independent experiments
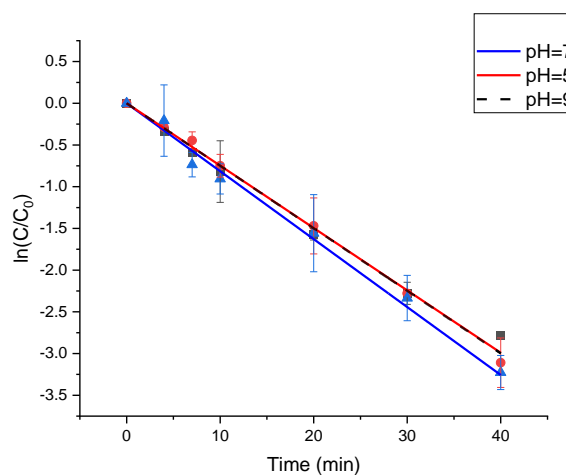
Figure 3.11 Geosmin removal kinetics in semi-batch at pH=5.0 (red), pH=7.0 (blue), pH=9.0 (black). (Methanol initial concentration=49 μM·L^{-1}, geosmin initial concentration≈20 μg·L^{-1}). Error bars indicate the standard deviation of the mean of three independent experiments
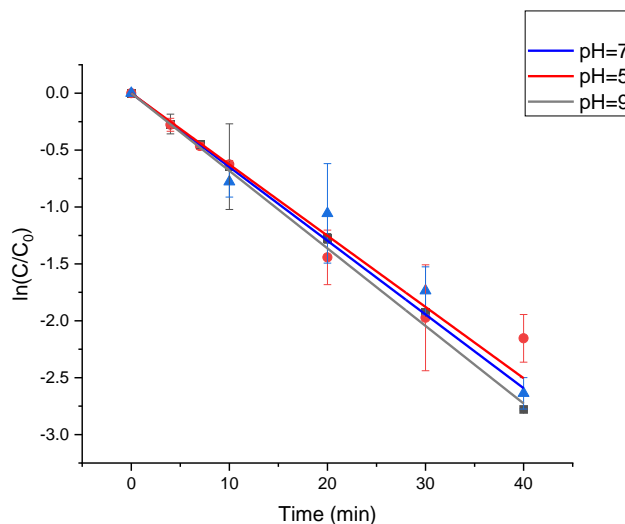
Figure 3.12 2-MIB removal kinetics in semi-batch at pH=5.0 (red), pH=7.0 (blue), pH=9.0 (black). (Methanol initial concentration=49 μM·L^{-1}, 2-MIB initial concentration≈25 μg·L^{-1}) Error bars indicate the standard deviation of the mean of three independent experiments

According to the equations (44) and (45), the experimental data in Fig. 3.7-3.9 are plotted in Fig. 3.10-3.12. In Fig.3.10, the linear regression coefficients (R^2) for pH of 5.0,7.0, and 9.0 are 0.855, 0.980 and 0.974 respectively.

Table 3.2 Rate constant values for geosmin or 2-MIB removal by semi-batch with different amounts of methanol

	Rate constant (min^{-1}) 1.48 μM·L^{-1} MeOH	Rate constant (min^{-1}) 49 μM·L^{-1} MeOH	
	Geosmin	Geosmin	2-MIB
pH =5.0	0.12389	0.05574	0.05325
pH =7.0	0.36022	0.06241	0.05544
pH =9.0	0.60448	0.05592	0.0588

It shows that the geosmin removal in a semi-batch reactor is close to a first-order reaction.

Similar results for geosmin and 2-MIB with the addition of methanol are shown in Fig. 3.11 and 3.12.

The rate constant values are shown in Table 3.2. They are derived from the apparent rate constant minus the rate regular of volatilization. Generally, the rate constant for 2-MIB is smaller than that of geosmin. It indicates that 2-MIB is more resistant to ozonation, probably due to higher tertiary carbons in the 2-MIB molecule (Liang et al., 2007).

3.4 Conclusion

The addition of H_2O_2 can enhance the H_2O_2/O_3 process by accelerating ozone decomposition, while ozonation treatment generally performs better in an alkaline environment.

Of the two target compounds, 2-MIB is more resistant than geosmin to ozonation, despite structural similarities.

The reaction in semi-batch reactors can act as an alternative method for H_2O_2/O_3 treatment giving enough reaction time. Hence the high H_2O_2 residual can be avoided.

Chapter 4

4.   Co-treatment of PF and PMS

In the previous study, ferrate (PF) alone has shown inefficiency in eliminating geosmin and 2-MIB (Liu et al., 2017, Park et al., 2007). However, another study observed the synergistic effect of PF and peroxymonosulfate (PMS). It is because PMS is powerful in generating $SO_4\cdot$, but PMS needs to be activated. The relationship between the treatment dosage and removal shows to be non-linear (Wu et al., 2018).

A Box-Behnken (BBD) was therefore applied to utilize response surface modeling (RSM). Moreover, BBD is an efficient method for experiment design. In BBD, the designed experimental combinations are at the midpoints of edges and center of the process space. Compared with central composite design, BBD requires fewer treatment combinations (Ferreira et al., 2007).

4.1 Experimental Materials

The standards of the target analyte geosmin (2 mg/mL) and potassium peroxymonosulfate (PMS, OXONE, $KHSO_5 \cdot 1/2KHSO_4 \cdot 1/2K_2SO_4$) were purchased from Sigma-Aldrich.

4.2   Experimental procedure

4.2.1   BBD

$20~\mu g \cdot L^{-1}$ GSM water samples were prepared in Milli-Q water from the standard solutions. The experiments of removal of geosmin and GSM in water samples were performed according to BBD. The pH is adjusted by 50 mM phosphate buffer.

50 mL of above water sample was placed in Erlenmeyer flasks stirred by hot plate at room temperature. Different dosages of PMS and PF were added to the water samples according to design. 10 mL sample was collected after 30 min. The collected sample was quenched by adding 10 μL of saturated sodium thiosulfate immediately. All experiments were conducted as triplicates.

The BBD scheme with three-factor and three-level for each factor was selected as the experiment design. A second-order polynomial equation was used to describe the removal efficiency versus the selected parameters based on previous studies, including solution pH (A), dosage of PMS (B) and PF(C). Table 4.1 shows the ranges and levels of the selected parameters.

Table 4.1 Ranges and levels of geosmin degradation of PF/PMS cotreatment experimental parameters (Geosmin initial concentration = 20 μg·L^{-1})

Variable	Ranges and levels		
	-1	0	+1
pH	5	7	9
PMS (mM)	0	5	10
PF (mM)	0	0.5	1

Design Expert 11.0 software was used to analyze responses and fit the data to mathematical models.

4.2.2 Kinetics

The kinetics study was conducted at the optimal point as predicted by the model derived through the BBD. The projected amount of PF and PMS was added to 100 mL of 20 μg·L^{-1} GSM solution. 10 mL sample was collected at 1, 5, 10, and 15 min. The collected sample was quenched by adding 10 μL of saturated sodium thiosulfate immediately. The experiments were conducted in duplicates.

4.3 Results and conclusion

4.3.1 Fitting of regression model equation

The removal efficiency of geosmin by PF and PMS co-treatment was calculated by the following equation (46)

$$Y(\%) = (C_0 - C_t)/C_0 * 100 \tag{46}$$

Where C_0 is the initial concentration of geosmin ($\mu g \cdot L^{-1}$); C_t is the geosmin concentration in solution after 30 min.

The regression model equation, including solution pH (A), PMS dosage (B), PF dosage (C), is listed as following equation (coded) (47).

$$Y=77.27+14.96*A+26.99*B+4.83*C-6.17*AB-3.78*BC-22.66*B^2 \tag{47}$$

Table 4.2 Experimental design matrix and experimental results of geosmin degradation by PF/PMS cotreatment (Geosmin initial concentration = 20 $\mu g \cdot L^{-1}$. Response is the mean of three independent experiments)

No.	Factor 1 A: pH	Factor 2 B: PMS	Factor 3 C: PF	Response 1 Geosmin removal (%)
1	-1	-1	0	8
2	0	0	0	78
3	1	1	0	88
4	0	-1	1	50
5	0	1	1	70
6	-1	0	1	68
7	0	-1	-1	6
8	1	0	-1	94
9	1	-1	0	46
10	0	1	-1	93
11	-1	0	-1	52
12	1	0	1	95
13	-1	1	0	75
14	0	0	0	78
15	0	0	0	77

4.3.2 Reliability analysis of the regression model equation

4.3.2.1 ANOVA tables

The significance and suitability of the model were examined by p-values of the analysis of variance (ANOVA). The ANOVA table (Table 4.3) for the response of removal of

geosmin shows the model is significant with a model F value of 258.70 and p-value<0.001. The result implies that there is a 0.01% chance that the F value occurs due to noise.

The significance of the individual coefficients and interactions shows that the terms including pH (A), the dosage of PMS (B) and PF (C), the interaction term including pH and PMS (AB), pH and PF (AC), and PMS and PF (BC) along with one quadratic coefficient (B^2) had the significant effect of the removal of geosmin (p<0.05).

Table 4.3 Analysis of variance (ANOVA) for the fit of geosmin removal efficiency from BBD by PF/PMS cotreatment (Geosmin initial concentration = 20 µg·L^{-1})

Source	Sum of Squares	df	Mean Square	F-value	p-value	
Model	11014.37	7	1573.481	258.7046	6.55E-08	significant
A-pH	1789.302	1	1789.302	294.1888	5.62E-07	
B-pms	5828.086	1	5828.086	958.2274	9.48E-09	
C-pf	186.3637	1	186.3637	30.64107	0.000873	
AB	152.1681	1	152.1681	25.01879	0.001562	
AC	57.29425	1	57.29425	9.420059	0.018088	
BC	1084.677	1	1084.677	178.3377	3.09E-06	
B^2	1916.478	1	1916.478	315.0986	4.44E-07	
Residual	42.57507	7	6.082154			
Lack of Fit	40.8115	5	8.162301	9.256565	0.100362	not significant
Pure Error	1.76357	2	0.881785			
Cor Total	11056.94	14				

4.3.2.2   Regression analysis

Table 4.4 Measure of statistical significance and adequate precision of BBD of 20 µg·L^{-1} geosmin removal by PF/PMS cotreatment

Std. Dev.	2.466202	R^2	0.996149
Mean	65.1855	Adjusted R^2	0.992299
C.V. %	3.78336	Predicted R^2	0.972411
		Adeq Precision	48.27103

The regression analysis is shown in Table 4.4. The model is suitable according to the R^2 values. Firstly, the actual R^2 value is close to 1, showing the strong correlation between independent variables and variants. Secondly, it is comparable to the adjusted R^2 value,

suggesting an insignificant influence of added terms. Thirdly, the slight difference between the predicted R^2 and adjusted R^2 shows a good prediction for new data with the model.

The adequate precision test measures the signal-to-noise ratio. It compares the range of the predicted values at the design points to the average prediction error. Ratios greater than 4 indicate adequate model discrimination. The adequate precision shows the adequate signal and implies that this model can be used to navigate the design space.

Furthermore, the low coefficient of variation (C.V.) shows the satisfactory precision and reliability of the experiment.
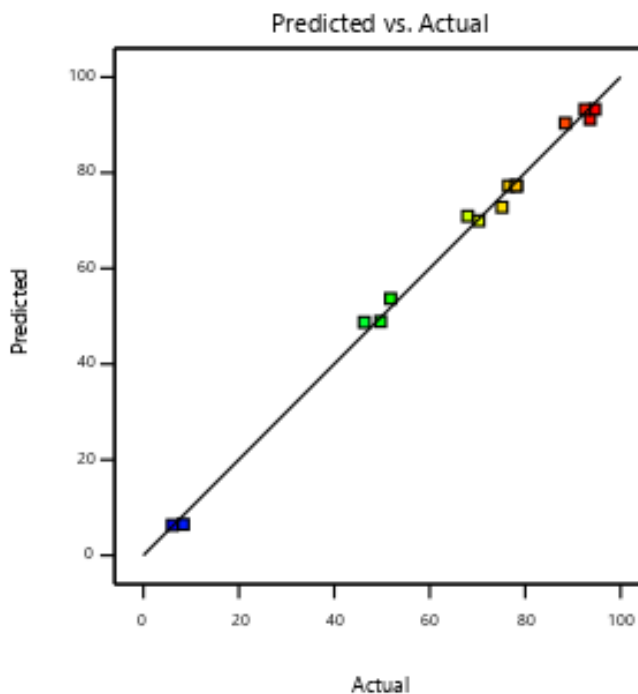
Figure 4.1 The observed values (%) plotted against the predicted values (%) derived from the geosmin removal BBD model by PF/PMS cotreatment

The experimental responses versus the predicted results are shown in Fig. 4.1. The predicted values are approximate to the experimental values.

4.3.3   Effect plots

The interactions among the variable factors are presented graphically in Fig. 4.2. The results indicate the combined effect of variables on geosmin removal. The figures are represented as a function of two factors holding the other factor at the center level. The response surface plot shows an elliptical or saddle shape, which implies significant interactions between the variables. But the interaction is fewer as it is not perfectly elliptical (Muralidhar et al., 2001).
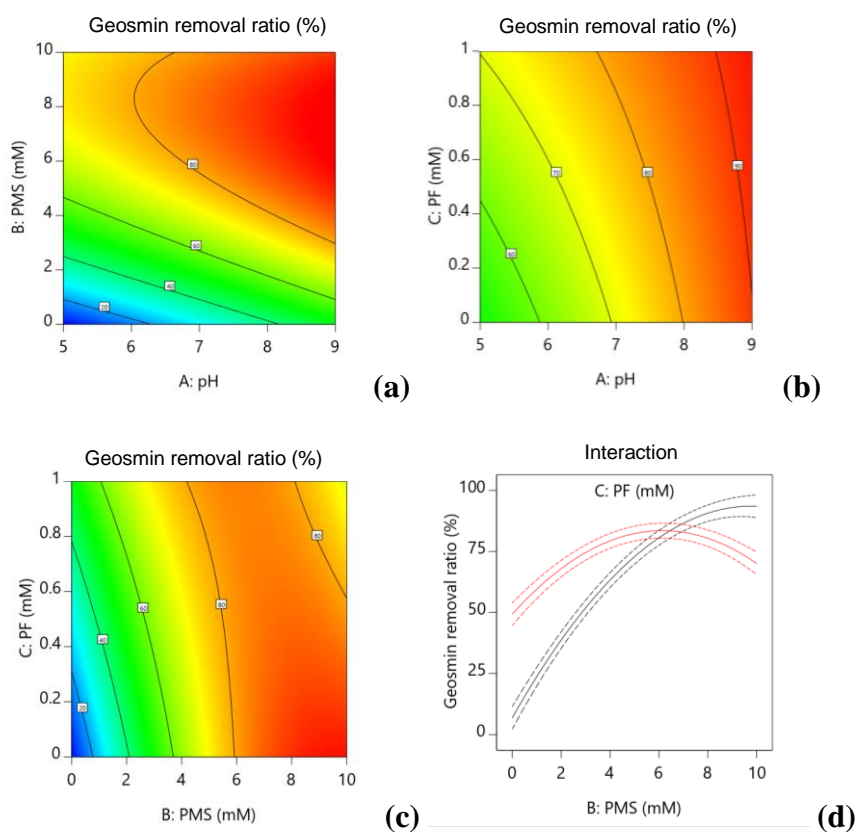
Figure 4.2 Contour plots and interactions of geosmin removal BBD by PF/PMS cotreatment (a) pH and PMS (b) pH and PF dosage (c) PMS and PF dosage (d) PF and PMS interaction

PMS & pH interaction

From the ANOVA table (table 4.3), the main effects of pH and the combined effects of pH with two other factors are all significant (p-values<0.05) for geosmin removal.

The increase of PMS dosage and solution pH leads to higher geosmin removal. The pH is important for the activation of PMS. PMS can decompose to generate radicals while the pH is between 7.0 and 11.0 (Ruiz et al., 2019). PMS decomposes as following equations: (Wang & Wang, 2018)

$$2HSO_5^- + H_2O \rightarrow H_2O_2 + HSO_4^- + H^+ + SO_5^{2-} \tag{48}$$

$$SO_5^{2-} + H_2O \rightarrow H_2O_2 + SO_4^{2-} \tag{49}$$

$$H_2O_2 + OH^- \rightarrow H_2O + HO_2^- \tag{50}$$

$$HSO_5^- + HO_2^- \rightarrow H_2O + \cdot SO_4^- + {}^1O_2 \tag{51}$$

$$H_2O_2 \rightarrow 2HO\cdot \tag{52}$$
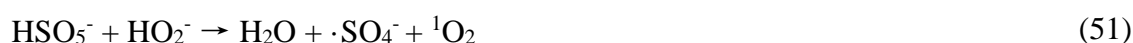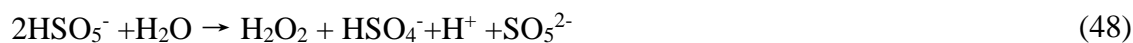
The equations show that in an alkaline environment, more HO· is produced. The study indicates that HO· counts for the degradation of geosmin two times higher than that of $SO_4^-\cdot$ (Xie et al., 2015). Moreover, at higher pH, other than $SO_4^-\cdot$, HO·, strong oxidants including $O_2^-\cdot$ and ${}^1O_2$ are also generated (Qi et al., 2016).

PF & pH interaction

Similar interaction of PF dosage and pH is also observed. The pH also influences the species after ferrate decomposition as the following equations (Wu et al., 2018):

$$H_3FeO_4^+ \rightarrow H^+ + H_2FeO_4 \text{ (pKa=1.6)} \tag{53}$$

$$H_2FeO_4 \rightarrow H^+ + HFeO_4^- \text{ (pKa=3.5)} \tag{54}$$

$$HFeO_4^- \rightarrow H^+ + FeO_4^{2-} \text{ (pKa=7.3)} \tag{55}$$
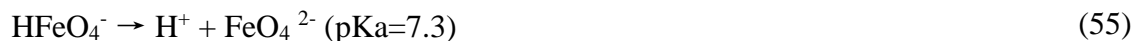
$HFeO_4^-$ is the major species at pH 3.5–7.3, and its reactivity is higher than that of FeO_4^{2-}. But the low degradation efficiency at this pH range shows geosmin is resistant to $HFeO_4^-$. Though FeO_4^{2-} is more stable at higher pH, it can also decompose as the equation (56) (Wu et al., 2018). the generated Fe $(OH)_3$ acts as a coagulant that removes more geosmin.

$$4 FeO_4^{2-} + 10 H_2O \rightarrow 4 Fe^{3+} + 3 O_2 + 20 OH^- \tag{56}$$

PMS & PF interaction

Fig.4.2 (d) shows the interaction of PMS and PF dosage. When PMS dosage is low, the increase of PMS and PF dosage is beneficial for geosmin removal. However, more PMS dosage results in a decrease in removal efficiency. A similar effect has been observed in the degradation of atrazine (Wu et al., 2018).

It can be explained by eliminating sulfate radicals by excessive PMS (Wu et al., 2018). Equation (51) shows decomposed PMS generates $SO_4^-\cdot$. However, abundant sulfate radicals react as equation (57) and (58) yield $S_2O_8^{2-}\cdot$ and $SO_5^-\cdot$, with redox potential of 2.01 and 1.10, respectively. In contrast, the redox potential of $SO_4^-\cdot$ is 2.60 (Oh et al., 2016), higher than these generated radicals. Therefore, the removal efficiency decreases with PMS overdose.

$$SO_4^-\cdot + SO_4^-\cdot \rightarrow S_2O_8^{2-}\cdot \qquad k=4.0 \times 10^8 \text{ M}^{-1}\text{ s}^{-1} \tag{57}$$

$$HSO_5^- + SO_4^-\cdot \rightarrow SO_5^-\cdot + HSO_4^-\cdot \qquad k< 10^5 \text{ M}^{-1}\text{s}^{-1} \tag{58}$$
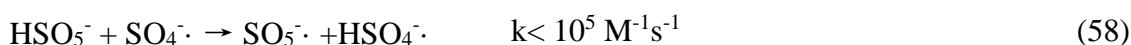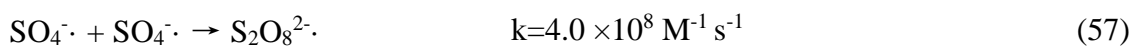
4.3.4 Empirical model validation

The confirmation results are shown in Table 4.5. A supplementary experimental run validated the optimized results and the quadratic models at an initial pH of 9.0. The experimental values obtained are shown in Table 4.6. The values were lower than LOQ, so the value was set at 0. The response of geosmin was comparable with the predicted response value.

Table 4.5 Parameters of PF and PMS co-treatment confirmation experiment

Factor	Name	Level	Low Level	High Level
A	pH	9	5	9
B	PMS	7.66	0	10
C	PF	0.24	0	1

Table 4.6 Results of PF and PMS co-treatment confirmation experiment

Response	Mean	Median [*]	Observed	Std Dev	n	SE Pred	95% PI low	Data Mean	95% PI high
gsm removal	100.90 37	100.903 7	100.0	2.4662 02	2	2.3848 52	95.26446	100	106.543

4.4 Reaction kinetics

The kinetics of PF and PMS co-treatment was analyzed, as shown in Fig.4.3. The data shows the co-treatment is very fast and completed in less than 1 min. This shows the addition of PF and PMS increased the concentration of radicals rapidly. It leads to the rapid degradation of geosmin. The slow reaction after the fast reaction phase may be due to the Fe $(OH)_3$ coagulation.
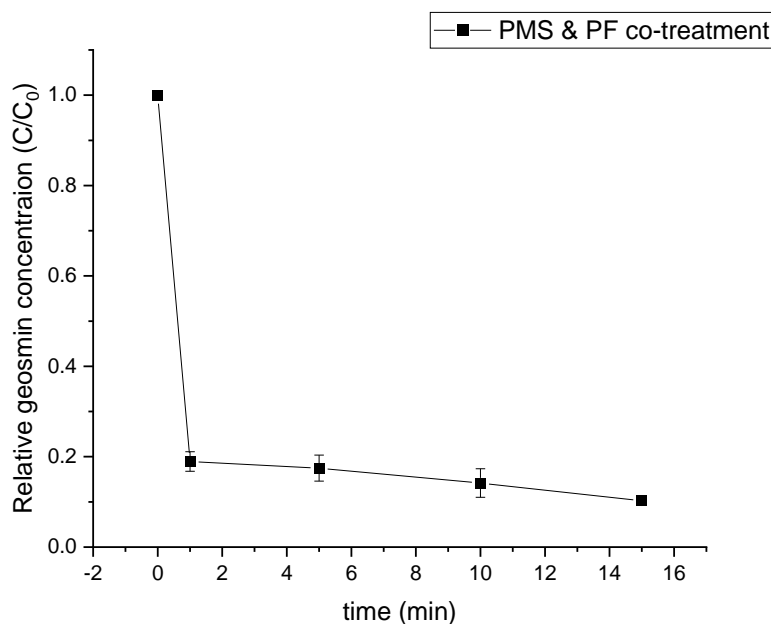
Figure 4.3 Kinetics study of PF/PMS co-treatment of geosmin (Geosmin initial concentration = 20 μg·L^{-1}, pH=9.0, PF=0.24 mM, PMS=7.66 mM) Error bars indicate the standard deviation of the mean of three independent experiments

4.5 Conclusion

The 3 factor BBD model can successfully predict geosmin removal over the tested parameter space, and overall, the co-treatment of PF and PMS can degrade geosmin efficiently. However, excessive PMS may hinder the reaction, so the PMS concentration needs to be selected carefully.

In a natural environment (pH 5-9), the dosage of PF/PMS co-treatment needs to be chosen based on the pH of the medium because of the strong interaction of pH with other parameters. The empirical model derived from the BBD experiment might be used as a basis for establishing treatment parameters under such conditions.

Chapter 5

5. Conclusions and Recommendations

5.1 Conclusions

The ozonation of geosmin and 2-MIB in the batch was not effective. However, the ozonation process can be enhanced by adding H_2O_2 and adjusting the pH to an alkaline environment. Nevertheless, the removal efficiency only increased to ~60%. Alternatively, sparging O_3 in the semi-batch reactor can achieve thorough removal of the target compounds. In addition, the scavenging effect of methanol for ozonation was observed.

Another AOP method, PF/PMS co-treatment, can remove geosmin completely. The empirical model derived from the 3 factor BBD within the selected parameter space can successfully predict the geosmin removal efficiency. For further application, the dosage of PF and PMS should be chosen according to the actual pH, the dominant parameter for removal efficiency.

In summary, both ozonation in semi-batch and the PF/PMS co-treatment can degrade the target compounds. However, PF/PMS co-treatment is more efficient considering the reaction time is much less and easier operation. However, the handling and storage of ferrate require more attention.

5.2 Recommendations

In chapter 3, the addition of H_2O_2 can be studied in the ozonation in a semi-batch to achieve better removal of T&O compounds in practical application. Moreover, a OH· kinetics study in ozonation can uncover the reaction efficiency. A common OH· probe, pCBA (4-chlorobenzoic acid), can determine the OH· concentration in water by HPLC.

From an academic perspective, the reaction pathway of PF/PMS co-treatment might yield additional information towards further optimization, and intermediate analysis via

GC/MS could yield valuable insight. The pathway analysis may also reveal the reason for low degradation efficiency of PF, which could show the limitation of PF treatment. In addition, scavenging tests can reveal the contribution of SO_4^- and OH· by adding correspondent scavengers, respectively.

Furthermore, similar experiments as presented here in surface water rather than Milli-Q water can shed light on the efficiency of this treatment in real conditions. Meanwhile, the separation of PF and PMS from the water after treatment is worthwhile to discover.

Bibliography

Aeree, T. E., Lee, C. Y., Butts, R. M., & Barnard, J. (1976). Geosmin, the Earthy Component of Table Beet Odor. *Journal of Agricultural and Food Chemistry*, *24*(2), 430–431.

Afsharnia, M., Kianmehr, M., Biglari, H., Dargahi, A., & Karimi, A. (2018). Disinfection of dairy wastewater effluent through solar photocatalysis processes. *Water Science and Engineering*, *11*(3), 214–219.

Agus, E., Zhang, L., & Sedlak, D. L. (2012). A framework for identifying characteristic odor compounds in municipal wastewater effluent. *Water Research*, *46*(18), 5970–5980.

Ahmad, W., Al-Sibaai, A. A., Bashammakh, A. S., Alwael, H., & El-Shahawi, M. S. (2015). Recent advances in dispersive liquid-liquid microextraction for pesticide analysis. *TrAC Trends in Analytical Chemistry*, *72*, 181–192.

Alaton, I. A., Akmehmet Balcioglu, I., & Bahnemann, D. W. (2002). Advanced oxidation of a reactive dyebath effluent: comparison of O_3 , H_2O_2 /UV-C and TiO_2 /UV-A processes. In *Water Research* (Vol. 36).

Aliaño-González, M., Ferreiro-González, M., Barbero, G., Palma, M., & Barroso, C. (2018). Application of Headspace Gas Chromatography-Ion Mobility Spectrometry for the Determination of Ignitable Liquids from Fire Debris. *Separations*, *5*(3), 41.

Bader, H., & Hoigne, J. (1982). Determination of ozone in water by the indigo method; a submitted standard method. *Ozone: Science & Engineering*, *4*(4), 169–176.

Bamuza-Pemu, E. E., & Chirwa, E. M. (2012). Photocatalytic degradation of geosmin: Reaction pathway analysis. *Water SA*, *38*(5), 689–696.

Bellu, E. (2007). Detection , analysis , and photocatalytic destruction of the freshwater taint compound geosmin. *Ph.D. Thesis*, *April*.

Beltran, F. J. (2003). *Ozone Reaction Kinetics for Water and Wastewater Systems - Fernando J. Beltran - Google Boeken*. CRC Press.

Burns, R. A., Crittenden, J. C., Hand, D. W., Selzer, V. H., Sutter, L. L., & Salman, S. R. (1999). Effect of Inorganic Ions in Heterogeneous Photocatalysis of TCE. *Journal of Environmental Engineering*, *125*(1), 77–85.

Callejón, R. M., Ubeda, C., Ríos-Reina, R., Morales, M. L., & Troncoso, A. M. (2016). Recent developments in the analysis of musty odour compounds in water and wine: A review. In *Journal of Chromatography A* (Vol. 1428, pp. 72–85).

Camara, M., Gharbi, N., Lenouvel, A., Behr, M., Guignard, C., Orlewski, P., & Evers, D. (2013). Detection and quantification of natural contaminants of wine by gas chromatography–differential ion mobility spectrometry (GC-DMS). *Journal of agricultural and food chemistry*, *61*(5), 1036-1043.

Chen, C., Yan, X., Yoza, B. A., Zhou, T., Li, Y., Zhan, Y., Wang, Q., & Li, Q. X. (2018). Efficiencies and mechanisms of ZSM5 zeolites loaded with cerium, iron, or manganese oxides for catalytic ozonation of nitrobenzene in water. *Science of the Total Environment*, *612*, 1424–1432.

Chen, S., Dong, B., Gao, K., & Li, T. (2019). Pilot study on advanced treatment of geosmin and 2-MIB with O_3/GAC. *Water Supply*, *19*(4), 1253-1263.

Chestnutt, T. E., Bach, M. T., & Mazyck, D. W. (2007). Improvement of thermal reactivation of activated carbon for the removal of 2-methylisoborneol. *Water Research*, *41*(1), 79–86.

Clercin, N. A. (2019). Origin and Fate of Odorous Metabolites, 2-methylisoborneol and Geosmin, in a Eutrophic Reservoir. In *Indiana University-Purdue University Indianapolis.* (Vol. 1, Issue 1).

Cook, D., Newcombe, G., & Sztajnbok, P. (2001). The application of powdered activated carbon for mib and geosmin removal: predicting PAC doses in four raw waters. *Water Research*, *35*(5), 1325–1333.

Cortada, C., Vidal, L., & Canals, A. (2011). Determination of geosmin and 2-methylisoborneol in water and wine samples by ultrasound-assisted dispersive liquid-liquid microextraction coupled to gas chromatography-mass spectrometry. *Journal of Chromatography. A*, *1218*(1), 17–22.

Cruz, M., Gomez, C., Duran-Valle, C. J., Pastrana-Martínez, L. M., Faria, J. L., Silva, A. M. T., Faraldos, M., & Bahamonde, A. (2017). Bare TiO_2 and graphene oxide TiO_2 photocatalysts on the degradation of selected pesticides and influence of the water matrix. *Applied Surface Science*, *416*, 1013–1021.

de Souza, S. M. de A. G. U., Bonilla, K. A. S., & de Souza, A. A. U. (2010). Removal of COD and color from hydrolyzed textile azo dye by combined ozonation and biological treatment. *Journal of Hazardous Materials*, *179*(1–3), 35–42.

Díez, A. M., Iglesias, O., Rosales, E., Sanromán, M. A., & Pazos, M. (2016). Optimization of two-chamber photo electro Fenton reactor for the treatment of winery wastewater. *Process Safety and Environmental Protection*, *101*, 72-79.

Dixon, Mike B., Falconet, C., Ho, L., Chow, C. W. K., O'Neill, B. K., & Newcombe, G. (2010). Nanofiltration for the removal of algal metabolites and the effects of fouling. *Water Science and Technology*, *61*(5), 1189–1199.

Dixon, Mike B., Falconet, C., Ho, L., Chow, C. W. K., O'Neill, B. K., & Newcombe, G. (2011). Removal of cyanobacterial metabolites by nanofiltration from two treated waters. *Journal of Hazardous Materials*, *188*(1–3), 288–295.

Dodds, W. K., Bouska, W. W., Eitzmann, J. L., Pilger, T. J., Pitts, K. L., Riley, A. J., Schloesser, J. T., & Thornbrugh, D. J. (2009). Eutrophication of U. S. freshwaters: Analysis of potential economic damages. *Environmental Science and Technology*, *43*(1), 12–19.

Doederer, K., De Vera, G. A., Espino, M. P., Pype, M.-L., Gale, D., & Keller, J. (2018). MIB and geosmin removal during adsorption and biodegradation phases of GAC filtration. *Water Supply*, *18*(4), 1449–1455.

Doederer, Katrin, Gale, D., & Keller, J. (2019). Effective removal of MIB and geosmin using MBBR for drinking water treatment. *Water Research*, *149*, 440–447.

Drikas, M., Dixon, M., & Morran, J. (2009). Removal of MIB and geosmin using granular activated carbon with and without MIEX pre-treatment. *Water Research*, *43*(20), 5151–5159.

El Hassani, K., Kalnina, D., Turks, M., Beakou, B. H., & Anouar, A. (2019). Enhanced degradation of an azo dye by catalytic ozonation over Ni-containing layered double hydroxide nanocatalyst. *Separation and Purification Technology*, *210*, 764–774.

Elkacmi, R., & Bennajah, M. (2019). Advanced oxidation technologies for the treatment and detoxification of olive mill wastewater: A general review. *Journal of Water Reuse and Desalination*, *9*(4), 463–505.

Ershov, B. G., & Morozov, P. A. (2009). The kinetics of ozone decomposition in water, the influence of pH and temperature. *Russian Journal of Physical Chemistry A 2009 83:8*, *83*(8), 1295–1299.

Farajzadeh, M. A., & Mogaddam, M. R. A. (2012). Air-assisted liquid-liquid microextraction method as a novel microextraction technique; Application in extraction and preconcentration of phthalate esters in aqueous sample followed by gas chromatography-flame ionization detection. *Analytica Chimica Acta*, *728*, 31–38.

Feng, M., Cizmas, L., Wang, Z., & Sharma, V. K. (2017). Synergistic effect of aqueous removal of fluoroquinolones by a combined use of peroxymonosulfate and ferrate(VI). *Chemosphere*, *177*, 144–148.

Feng, Y., Smith, D. W., & Bolton, J. R. (2007). Photolysis of aqueous free chlorine species (HOCl and OCl-) with 254 nm ultraviolet light. *Journal of Environmental Engineering and Science*, *6*(3), 277–284.

Ferreira, S. L. C., Bruns, R. E., Ferreira, H. S., Matos, G. D., David, J. M., Brandão, G. C., da Silva, E. G. P., Portugal, L. A., dos Reis, P. S., Souza, A. S., & dos Santos,

W. N. L. (2007). Box-Behnken design: An alternative for the optimization of analytical methods. In *Analytica Chimica Acta* (Vol. 597, Issue 2, pp. 179–186).

Fischbacher, A., von Sonntag, J., von Sonntag, C., & Schmidt, T. C. (2013). The• OH radical yield in the H_2O_2+ O_3 (peroxone) reaction. *Environmental science & technology*, *47*(17), 9959-9964.

Fotiou, T., Triantis, T. M., Kaloudis, T., & Hiskia, A. (2015). Evaluation of the photocatalytic activity of TiO_2 based catalysts for the degradation and mineralization of cyanobacterial toxins and water off-odor compounds under UV-A, solar and visible light. *Chemical Engineering Journal*, *261*, 17–26.

Fotiou, Theodora, Triantis, T. M., Kaloudis, T., O'Shea, K. E., Dionysiou, D. D., & Hiskia, A. (2016). Assessment of the roles of reactive oxygen species in the UV and visible light photocatalytic degradation of cyanotoxins and water taste and odor compounds using C–TiO_2. *Water Research*, *90*, 52–61.

Gogate, P. R., & Pandit, A. B. (2004). A review of imperative technologies for wastewater treatment II: Hybrid methods. *Advances in Environmental Research*, *8*(3–4), 553–597.

Guo, Q., Yu, J., Yang, K., Wen, X., Zhang, H., Yu, Z., ... & Yang, M. (2016). Identification of complex septic odorants in Huangpu River source water by combining the data from gas chromatography-olfactometry and comprehensive two-dimensional gas chromatography using retention indices. *Science of the Total Environment*, *556*, 36-44.

Gupta, S., Gomaa, H., & Ray, M. B. (2021). A novel submerged photocatalytic oscillatory membrane reactor for water polishing. *Journal of Environmental Chemical Engineering*, *9*(4), 105562.

H. Wee, L., Nikki Janssens, Jeori Vercammen, Lorenzo Tamaraschi, J. Thomassen, L. C., & A. Martens, J. (2015). Stable TiO_2 –USY zeolite composite coatings for efficient adsorptive and photocatalytic elimination of geosmin from water. *Journal of*

Materials Chemistry A, *3*(5), 2258–2264.

Handy, R., Barnelt, D. A., Purves, R. W., Horlick, G., & Guevremont, R. (2000). Determination of nanomolar levels of perchlorate in water by ESIFAIMS-MS. *Journal of Analytical Atomic Spectrometry*, *15*(8), 907–911.

He, X., De La Cruz, A. A., & Dionysiou, D. D. (2013). Destruction of cyanobacterial toxin cylindrospermopsin by hydroxyl radicals and sulfate radicals using UV-254 nm activation of hydrogen peroxide, persulfate and peroxymonosulfate. *Journal of Photochemistry and Photobiology A: Chemistry*, *251*, 160–166.

Ho, L., Hoefel, D., Bock, F., Saint, C. P., & Newcombe, G. (2007). Biodegradation rates of 2-methylisoborneol (MIB) and geosmin through sand filters and in bioreactors. *Chemosphere*, *66*(11), 2210–2218.

Houle, S., Schrader, K. K., Le Franccois, N. R., Comeau, Y., Kharoune, M., Summerfelt, S. T., Savoie, A., & Vandenberg, G. W. (2011). Geosmin causes off-flavour in arctic charr in recirculating aquaculture systems. *Aquaculture Research*, *42*(3), 360–365.

Howgate, P. (2004). Tainting of farmed fish by geosmin and 2-methyl-iso-borneol: a review of sensory aspects and of uptake/depuration. *Aquaculture*, *234*(1–4), 155–181.

Hsieh, S. T., Lin, T. F., & Wang, G. S. (2010). Biodegradation of MIB and geosmin with slow sand filters. *Journal of Environmental Science and Health - Part A Toxic/Hazardous Substances and Environmental Engineering*, *45*(8), 951–957.

Ioannou, L., Velegraki, T., Michael, C., Mantzavinos, D., & Fatta-Kassinos, D. (2013). Sunlight, iron and radicals to tackle the resistant leftovers of biotreated winery wastewater. *Photochemical and Photobiological Sciences*, *12*(4), 664–670.

Jeleń, H. H., Majcher, M., Zawirska-Wojtasiak, R., Wiewiórowska, M., & Wąsowicz, E. (2003). Determination of geosmin, 2-methylisoborneol, and a musty-earthy odor in wheat grain by SPME-GC-MS, profiling volatiles, and sensory analysis. *Journal of Agricultural and food Chemistry*, *51*(24), 7079-7085.

Jiang, J. Q., & Lloyd, B. (2002). Progress in the development and use of ferrate(VI) salt as an oxidant and coagulant for water and wastewater treatment. *Water Research*, *36*(6), 1397–1408.

Jo, C. H., Dietrich, A. M., & Tanko, J. M. (2011). Simultaneous degradation of disinfection byproducts and earthy-musty odorants by the UV/H_2O_2 advanced oxidation process. *Water Research*, *45*(8), 2507–2516.

Jo, C. H. (2008). *Oxidation of Disinfection Byproducts and Algae-related Odorants by UV/H_2O_2* (Doctoral dissertation, Virginia Tech).

Khataee, A., Vahid, B., Behjati, B., Safarpour, M., & Joo, S. W. (2014). Kinetic modeling of a triarylmethane dye decolorization by photoelectro-Fenton process in a recirculating system: Nonlinear regression analysis. *Chemical Engineering Research and Design*, *92*(2), 362–367.

Kim, C., Lee, S. Il, Hwang, S., Cho, M., Kim, H. S., & Noh, S. H. (2014). Removal of geosmin and 2-methylisoboneol (2-MIB) by membrane system combined with powdered activated carbon (PAC) for drinking water treatment. *Journal of Water Process Engineering*, *4*(C), 91–98.

Kim, T.-K., Moon, B.-R., Kim, T., Kim, M.-K., & Zoh, K.-D. (2016). Degradation mechanisms of geosmin and 2-MIB during UV photolysis and UV/chlorine reactions. *Chemosphere*, *162*, 157–164.

Kimstach, y D. C. and V. (1992). *Water Quality Assessments-A Guide to Use of Biota, Sediments and Water in Environmental Monitoring-Second Edition Chapter 3*- Selection of water quality variables*.

Klausen, M. M., & Grønborg, O. (2010). Pilot scale testing of advanced oxidation processes for degradation of geosmin and MIB in recirculated aquaculture. *Water Supply*, *10*(2), 217–225.

Kocúrová, L., Balogh, I. S., Šandrejová, J., & Andruch, V. (2012). Review article. *Microchemical Journal*, *Complete*(102), 11–17.

Krzemińska, D., Neczaj, E., & Borowski, G. (2015). Advanced oxidation processes for food industrial wastewater decontamination. *Journal of Ecological Engineering*, *16*(2), 61–71.

Lalezary-Craig, S., Pirbazari, M., Dale, M. S., Tanaka, T. S., & McGuire, M. J. (1988). Optimizing the Removal of Geosmin and 2-Methylisoborneol by Powdered Activated Carbon. *Journal - American Water Works Association*, *80*(4), 73–80.

Lee, K., Paterson, A., … J. P.-J. of the I., & 2001, U. (2001). Origins of flavour in whiskies and a revised flavour wheel: a review. *Wiley Online Library*, *107*(5), 287–313.

Li, Y. (2015). *Estimating the Remaining GAC Removal Capacity for Geosmin and MIB*. University of Toronto (Canada).

Liang, C., Wang, D., Chen, J., Zhu, L., & Yang, M. (2007). Kinetics analysis on the ozonation of MIB and geosmin. *Ozone: Science and Engineering*, *29*(3), 185–189.

Ling, S. K., Wang, S., & Peng, Y. (2010). Oxidative degradation of dyes in water using Co^{2+}/H_2O_2 and Co^{2+}/peroxymonosulfate. *Journal of Hazardous Materials*, *178*(1–3), 385–389.

Liu, S., Tang, L., Wu, M., Fu, H. Z., Xu, J., Chen, W., & Ma, F. (2017). Parameters influencing elimination of geosmin and 2-methylisoborneol by K2FeO4. *Separation and Purification Technology*, *182*, 128–133.

Long, T. C., Saleh, N., Tilton, R. D., Lowry, G. V., & Veronesi, B. (2006). Titanium dioxide (P25) produces reactive oxygen species in immortalized brain microglia (BV2): implications for nanoparticle neurotoxicity. *Environmental science & technology*, *40*(14), 4346-4352.

Lu, G., Fellman, J. K., Edwards, C. G., Mattinson, D. S., & Navazio, J. (2003). Quantitative determination of geosmin in red beets (Beta vulgaris L.) using headspace solid-phase microextraction. *Journal of Agricultural and Food Chemistry*, *51*(4), 1021–1025.

Luo, G., Wang, J., Ma, N., Liu, Z., & Tan, H. (2016). Effects of inoculated Bacillus subtilis on geosmin and 2-methylisoborneol removal in suspended growth reactors using aquacultural waste for biofloc production. *Journal of Microbiology and Biotechnology*, *26*(8), 1420–1427.

Ma, L., Wang, C., Li, H., Peng, F., & Yang, Z. (2018). Degradation of geosmin and 2-methylisoborneol in water with UV/chlorine: Influencing factors, reactive species, and possible pathways. *Chemosphere*, *211*, 1166–1175.

Ma, X., Gao, N., Chen, B., Li, Q., Zhang, Q., & Gu, G. (2007). Detection of geosmin and 2-methylisoborneol by liquid-liquid extraction-gas chromatograph mass spectrum (LLE-GCMS) and solid phase extraction-gas chromatograph mass spectrum (SPE-GCMS). *Frontiers of Environmental Science and Engineering in China*, *1*(3), 286–291.

Matsui, Y., Ando, N., Sasaki, H., Matsushita, T., & Ohno, K. (2009). Branched pore kinetic model analysis of geosmin adsorption on super-powdered activated carbon. *Water Research*, *43*(12), 3095–3103.

Matsui, Y., Nakao, S., Sakamoto, A., Taniguchi, T., Pan, L., Matsushita, T., & Shirasaki, N. (2015). Adsorption capacities of activated carbons for geosmin and 2-methylisoborneol vary with activated carbon particle size: Effects of adsorbent and adsorbate characteristics. *Water Research*, *85*, 95–102.

McDowall, B., Hoefel, D., Newcombe, G., Saint, C. P., & Ho, L. (2009). Enhancing the biofiltration of geosmin by seeding sand filter columns with a consortium of geosmin-degrading bacteria. *Water Research*, *43*(2), 433–440.

Melwanki, M. B., & Fuh, M. R. (2008). Dispersive liquid-liquid microextraction combined with semi-automated in-syringe back extraction as a new approach for the sample preparation of ionizable organic compounds prior to liquid chromatography. *Journal of Chromatography A*, *1198–1199*(1–2), 1–6.

Miklos, D. B., Remy, C., Jekel, M., Linden, K. G., Drewes, E., & Hübner, U. (2018).

Review Evaluation of advanced oxidation processes for water and wastewater treatment e A critical review. *Water Research*, *139*, 118–131.

Mizuno, T., Ohara, S., Nishimura, F., & Tsuno, H. (2011). O₃/H₂O₂ Process for Both Removal of Odorous Algal-Derived Compounds and Control of Bromate Ion Formation. *33*(2), 121–135.

Mosteo, R., Ormad, P., Mozas, E., Sarasa, J., & Ovelleiro, J. L. (2006). Factorial experimental design of winery wastewaters treatment by heterogeneous photo-Fenton process. Water Research, 40(8), 1561-1568.

Munter, R. (2001). Advanced Oxidation Processes-Current Status and Prospects: Proceedings of Estonian Academy of Sciences. *Chemistry*, *50*, 59–80.

Muralidhar, R. V., Chirumamila, R. R., Marchant, R., & Nigam, P. (2001). A response surface approach for the comparison of lipase production by Candida cylindracea using two different carbon sources. *Biochemical Engineering Journal*, *9*(1), 17–23.

Nam-Koong, H., Schroeder, J. P., Petrick, G., & Schulz, C. (2016). Removal of the off-flavor compounds geosmin and 2-methylisoborneol from recirculating aquaculture system water by ultrasonically induced cavitation. *Aquacultural Engineering*, *70*, 73–80.

Nerenberg, R., Rittmann, B. E., & Soucie, W. J. (2000). Ozone/biofiltration for removing MIB and geosmin. *Journal - American Water Works Association*, *92*(12), 85–95.

Newcombe, G., Morrison, J., Hepplewhite, C., & Knappe, D. R. U. (2002). In the (adsorption) competition between NOM and MIB, who is the winner, and why? *Water Science and Technology: Water Supply*, *2*(2), 59–67.

Oh, W. Da, Dong, Z., & Lim, T. T. (2016). Generation of sulfate radical through heterogeneous catalysis for organic contaminants removal: Current development, challenges and prospects. In *Applied Catalysis B: Environmental* (Vol. 194, pp. 169–201). Elsevier B.V.

Olmez-Hanci, T., & Arslan-Alaton, I. (2013). Comparison of sulfate and hydroxyl radical based advanced oxidation of phenol. *Chemical Engineering Journal*, *224*(1), 10–16.

Ormad, M. P., Mosteo, R., Ibarz, C., & Ovelleiro, J. L. (2006). Multivariate approach to the photo-Fenton process applied to the degradation of winery wastewaters. *Applied Catalysis B: Environmental*, *66*(1-2), 58-63.

Park, G., Yu, M., Go, J., Kim, E., & Kim, H. (2007). Comparison between ozone and ferrate in oxidising geosmin and 2-MIB in water. *Water Science and Technology*, *55*(5), 117–125.

Park, G., Yu, M., Koo, J. Y., Joe, W. H., & Kim, H. (2006). Oxidation of geosmin and MIB in water using O_3/H_2O_2: Kinetic evaluation. *Water Science and Technology: Water Supply*, *6*(2), 63–69.

Park, J. A., Nam, H. L., Choi, J. W., Ha, J., & Lee, S. H. (2017). Oxidation of geosmin and 2-methylisoborneol by the photo-Fenton process: Kinetics, degradation intermediates, and the removal of microcystin-LR and trihalomethane from Nak-Dong River water, South Korea. *Chemical Engineering Journal*, *313*, 345–354.

Pestana, C. J., Lawton, L. A., & Kaloudis, T. (2020). Removal and/or Destruction of Cyanobacterial Taste and Odour Compounds by Conventional and Advanced Oxidation Processes. In *Water Treatment for Purification from Cyanobacteria and Cyanotoxins* (pp. 207–230).

Peter, A., & Von Gunten, U. (2007). Oxidation kinetics of selected taste and odor compounds during ozonation of drinking water. *Environmental Science and Technology*, *41*(2), 626–631.

Pettit, S. L., Rodriguez-Gonzalez, L., Michaels, J. T., Alcantar, N. A., Ergas, S. J., & Kuhn, J. N. (2014). Parameters influencing the photocatalytic degradation of geosmin and 2-methylisoborneol utilizing immobilized TiO_2. *Catalysis Letters*, *144*(8), 1460–1465.

Prasetyaningrum, A., Kusumaningtyas, D. A., Suseno, P., & Ratnawati, R. (2019). Effect

of pH and Gas Flow Rate on Ozone Mass Transfer of K-Carrageenan Solution in Bubble Column Reactor. *Reaktor*, *18*(04), 177–182.

Qi, C., Liu, X., Ma, J., Lin, C., Li, X., & Zhang, H. (2016). Activation of peroxymonosulfate by base: Implications for the degradation of organic pollutants. *Chemosphere*, *151*, 280–288.

Quigley, A., Cummins, W., & Connolly, D. (2016). Dispersive liquid-liquid microextraction in the analysis of milk and dairy products: A review. *Journal of Chemistry*, *2016*.

Riaz, S., & Park, S. J. (2020). An overview of TiO$_2$-based photocatalytic membrane reactors for water and wastewater treatments. *Journal of Industrial and Engineering Chemistry*, *84*, 23–41.

Rittmann, B. (1995). Biological treatment to control tadte-and-odor compounds in drinking water treatment. *Advances in Taste-and-Odor Treatment and Control*, 203–240.

Rodriguez-Gonzalez, L., Pettit, S. L., Zhao, W., Michaels, J. T., Kuhn, J. N., Alcantar, N. A., & Ergas, S. J. (2019). Oxidation of off flavor compounds in recirculating aquaculture systems using UV-TiO$_2$ photocatalysis. *Aquaculture*, *502*, 32–39.

Romero, J., Manero, I., & Laso, J. (2007). Validation of geosmin and 2-methyl-i-borneol analysis by CLSA-GC-FID method to obtain ISO-17025 accreditation. *Journal of Chromatographic Science*, *45*(7), 439–446.

Rosenfeldt, E. J., Melcher, B., & Linden, K. G. (2005). UV and UV/H$_2$O$_2$ treatment of methylisoborneol (MIB) and geosmin in water. *Journal of Water Supply: Research and Technology-Aqua*, *54*(7), 423–434.

Ruiz, M., Yang, Y., Lochbaum, C. A., Delafield, D. G., Pignatello, J. J., Li, L., & Pedersen, J. A. (2019). Peroxymonosulfate Oxidizes Amino Acids in Water without Activation. *Environmental Science & Technology*, *53*(18), 10845–10854.

Saito, A., Tokuyama, T., Tanaka, A., Oritani, T., & Fuchigami, K. (1999). Microbiological degradation of (-)-geosmin. *Water Research*, *33*(13), 3033–3036.

Goldstein, S., Aschengrau, D., Diamant, Y., & Rabani, J. (2007). Photolysis of aqueous H_2O_2: quantum yield and applications for polychromatic UV actinometry in photoreactors. *Environmental science & technology*, *41*(21), 7486-7490.

Sarayu, K., Swaminathan, K., & Sandhya, S. (2007). Assessment of degradation of eight commercial reactive azo dyes individually and in mixture in aqueous solution by ozonation. *Dyes and Pigments*, *75*(2), 362–368.

Scharf, R. G., Johnston, R. W., Semmens, M. J., & Hozalski, R. M. (2010). Comparison of batch sorption tests, pilot studies, and modeling for estimating GAC bed life. *Water Research*, *44*(3), 769–780.

Schrader, K. K., Davidson, J. W., Rimando, A. M., & Summerfelt, S. T. (2010). Evaluation of ozonation on levels of the off-flavor compounds geosmin and 2-methylisoborneol in water and rainbow trout Oncorhynchus mykiss from recirculating aquaculture systems. *Aquacultural Engineering*, *43*(2), 46–50.

Sehested, K., Corfltzen, H., Holcman, J., Fischer, C. H., & Hart, E. J. (1991). Standard Methods for the Examination of Water and Wastewater. In *C. T. Reactions and Movement of Organic Chemicals in Soils. SSSA Spec. Publ* (Vol. 25, Issue 8).

Sharma, V. K. (2002). Potassium ferrate(VI): an environmentally friendly oxidant. *Advances in Environmental Research*, *6*(2), 143–156.

Song, W., & O'Shea, K. E. (2007). Ultrasonically induced degradation of 2-methylisoborneol and geosmin. *Water Research*, *41*(12), 2672-2678.

Staehelin, J., & Holgné, J. (1982). Decomposition of Ozone in Water: Rate of Initiation by Hydroxide Ions and Hydrogen Peroxide. *Environmental Science and Technology*, *16*(10), 676–681.

Sushma, Kumari, M., & Saroha, A. K. (2018). Performance of various catalysts on

treatment of refractory pollutants in industrial wastewater by catalytic wet air oxidation: A review. In *Journal of Environmental Management* (Vol. 228, pp. 169–188).

Tian, L., Gu, R., Han, F., Huang, D., Shi, Y., Lou, X., & Cai, Y. (2017). Determination of geosmin and 2-methylisoborneol in source water by dispersive liquid-liquid micro-extraction combined with gas chromatography-mass spectrometry. *Proceedings of the 2017 6th International Conference on Energy and Environmental Protection (ICEEP 2017)*, *143*(Iceep), 646–650.

Tully, F. P., Droege, A. T., Koszykowski, M. L., & Melius, C. F. (1986). Hydrogen-atom abstraction from alkanes by OH. 2. Ethane. *Journal of Physical Chemistry*, *90*(4), 691–698.

Vautz, W., Baumbach, J. I., & Jung, J. (2004). Continuous Monitoring of the Fermentation of Beer By Ion Mobility Spectrometry. *International Journal for Ion Mobility Spectrometry*, *7*(2), 3–5.

Wang, D., Bolton, J. R., Andrews, S. A., & Hofmann, R. (2015). UV/chlorine control of drinking water taste and odour at pilot and full-scale. *Chemosphere*, *136*, 239–244.

Wang, D., Bolton, J. R., & Hofmann, R. (2012). Medium pressure UV combined with chlorine advanced oxidation for trichloroethylene destruction in a model water. *Water Research*, *46*(15), 4677–4686.

Wang, Jianlong, & Bai, Z. (2017). Fe-based catalysts for heterogeneous catalytic ozonation of emerging contaminants in water and wastewater. In *Chemical Engineering Journal* (Vol. 312, pp. 79–98).

Wang, Jianlong, & Wang, S. (2018). Activation of persulfate (PS) and peroxymonosulfate (PMS) and application for the degradation of emerging contaminants. *Chemical Engineering Journal*, *334*(November), 1502–1517.

Wang, Jing, Cui, H., Xie, G., Liu, B., Cao, G., & Xing, D. (2020). Co-treatment of potassium ferrate and peroxymonosulfate enhances the decomposition of the cotton

straw and cow manure mixture. *Science of the Total Environment*, *724*, 138321.

Watson, S. B., Ridal, J., Boyer, G. L., Watson, S., Ridal Saint Lawrence, J., & Boyer, G. (2008). Taste and odour and cyanobacterial toxins: impairment, prediction, and management in the Great Lakes. *Can. J. Fish. Aquat. Sci*, *65*, 1779–1796.

Watts, M. J., & Linden, K. G. (2007). Chlorine photolysis and subsequent OH radical production during UV treatment of chlorinated water. *Water Research*, *41*(13), 2871–2878.

Westerhoff, P., Nalinakumari, B., & Pei, P. (2006). Kinetics of MIB and geosmin oxidation during ozonation. *Ozone: Science and Engineering*, *28*(5), 277–286.

Wu, S., Li, H., Li, X., He, H., & Yang, C. (2018). Performances and mechanisms of efficient degradation of atrazine using peroxymonosulfate and ferrate as oxidants. *Chemical Engineering Journal*, *353*, 533–541.

Xia, P., Zhang, S., Yu, J., Ye, H., Zhang, D., Jiang, L., Wang, Z., & Yin, D. (2020). Complex odor control based on ozonation/GAC advanced treatment: optimization and application in one full-scale water treatment plant. *Environmental Sciences Europe*, *32*(1).

Xia, T., Kovochich, M., Brant, J., Hotze, M., … J. S.-N., & 2006, undefined. (2006). Comparison of the abilities of ambient and manufactured nanoparticles to induce cellular toxicity according to an oxidative stress paradigm. *ACS Publications*, *6*(8), 1794–1807.

Xie, P., Ma, J., Liu, W., Zou, J., Yue, S., Li, X., Wiesner, M. R., & Fang, J. (2015). Removal of 2-MIB and geosmin using UV/persulfate: Contributions of hydroxyl and sulfate radicals. *Water Research*, *69*, 223–233.

Xue, Q., Liu, Y., Zhou, Q., Utsumi, M., Zhang, Z., & Sugiura, N. (2016). Photocatalytic degradation of geosmin by Pd nanoparticle modified WO_3 catalyst under simulated solar light. *Chemical Engineering Journal*, *283*, 614–621.

Xue, Q., Shimizu, K., Sakharkar, M. K., Utsumi, M., Cao, G., Li, M., Zhang, Z., & Sugiura, N. (2012). Geosmin degradation by seasonal biofilm from a biological treatment facility. *Environmental Science and Pollution Research*, *19*(3), 700–707.

Yao, W., Qu, Q., von Gunten, U., Chen, C., Yu, G., & Wang, Y. (2017a). Comparison of methylisoborneol and geosmin abatement in surface water by conventional ozonation and an electro-peroxone process. *Water Research*, *108*, 373–382.

Yaparatne, S., Tripp, C. P., & Amirbahman, A. (2018). Photodegradation of taste and odor compounds in water in the presence of immobilized TiO 2 -SiO 2 photocatalysts. *Journal of Hazardous Materials*, *346*, 208–217.

Yuan, B., Xu, D., Li, F., & Fu, M.-L. (2013). Removal efficiency and possible pathway of odor compounds (2-methylisoborneol and geosmin) by ozonation. *Separation and Purification Technology*, *117*, 53–58.

Yuan, R., Wang, S., Liu, D., Shao, X., & Zhou, B. (2018). Effect of the wavelength on the pathways of 2-MIB and geosmin photocatalytic oxidation in the presence of Fe-N co-doped TiO_2. *Chemical Engineering Journal*, *353*, 319–328.

Zamyadi, A., Henderson, R., Stuetz, R., Hofmann, R., Ho, L., & Newcombe, G. (2015). Fate of geosmin and 2-methylisoborneol in full-scale water treatment plants. *Water Research*, *83*, 171–183.

Zat, M., & Benetti, A. D. (2011). Remoção dos compostos odoríferos geosmina e 2-metilisoborneol de águas de abastecimento através de processos de aeração em cascata, dessorção por ar e nanofiltração. *Engenharia Sanitaria e Ambiental*, *16*(4), 353–360.

Zgoła-Grześkowiak, A., & Grześkowiak, T. (2011). Dispersive liquid-liquid microextraction. *TrAC Trends in Analytical Chemistry*, *30*(9), 1382–1399.

Zhang, T., Xue, Y., Li, Z., Wang, Y., Yang, W., & Xue, C. (2016). Effects of ozone on the removal of geosmin and the physicochemical properties of fish meat from bighead carp (Hypophthalmichthys Nobilis). *Innovative Food Science and Emerging*

Technologies, *34*, 16–23.

Zhao, W., Zhang, Y., Rodriguez-Gonzalez, L. C., Zhong, F., Ergas, S. J., & Alcantar, N. A. (2015). Removal of Off-Flavor Compounds in Aquaculture Water by Spray-Coated TiO 2 Photocatalysis. *J Chem Eng Process Technol*, *6*(3), 237.

Zheng, X., Shen, Z. P., Shi, L., Cheng, R., & Yuan, D. H. (2017). Photocatalytic membrane reactors (PMRs) in water treatment: Configurations and influencing factors. *Catalysts*, *7*(8).

Zoschke, K., Dietrich, N., Börnick, H., & Worch, E. (2012). UV-based advanced oxidation processes for the treatment of odour compounds: Efficiency and by-product formation. *Water Research*, *46*(16), 5365–5373.

Zoschke, K., Engel, C., Börnick, H., & Worch, E. (2011). Adsorption of geosmin and 2-methylisoborneol onto powdered activated carbon at non-equilibrium conditions: Influence of NOM and process modeling. *Water Research*, *45*(15), 4544–4550.

Zuo, Y., Li, L., Wu, Z., & Song, L. (2009). Isolation, identification and odour-producing abilities of geosmin/2-MIB in actinomycetes from sediments in Lake Lotus, China. *Journal of Water Supply: Research and Technology - AQUA*, *58*(8), 552–561.

Curriculum Vitae

Name: Zhaoran Xin

Post-secondary   East China University of Sci. & Tech.
Education and   Shanghai, China
Degrees: 2015-2019 B.A.

                     The University of Western Ontario
                     London, Ontario, Canada
                     2019-2021 M.E.Sc

Related Work   Teaching Assistant
Experience   The University of Western Ontario
                    2020-2021

Publications:
Xin, Z., & Rehmann, L. (2020). Application of Advanced Oxidation Process in the Food Industry. *Advanced Oxidation Processes*, 101.